Inter-annual memory effects between Soil Moisture and NDVI in the Sahel

Yang Zhou
June, 2013

Inter-annual memory effects between Soil Moisture and NDVI in the Sahel

by

Yang Zhou

Thesis submitted to the Department of Physical Geography and Ecosystem Science of Lund University in partial fulfilment of the requirements for the degree of Master of Science in Geo-information Science and Earth Observation for Environmental Modelling and Management.

Thesis Assessment Board

Professor Lars Eklundh
Professor Petter Pilesjö
Ass. Professor Jonathan Seaquist

Lund University GEM thesis series nr 3

Disclaimer

This document describes work undertaken as part of a programme of study at the Faculty of Geo-information Science and Earth Observation (ITC) of the University of Twente and the Department of Physical Geography and Ecosystem Science of Lund University. All views and opinions expressed therein remain the sole responsibility of the author, and do not necessarily represent those of the institute.

Abstract

The Sahel lies in the semi-arid zone of North Africa between the Sahara Desert to the north and the savannas and rainforest to the south. In the Sahel, the variability of vegetation growth is predominately controlled by moisture reception in the concurrent rainy season. The inter-annual variability of normalized difference vegetation index (NDVI) during the rainy season (April to August) can be explained very well by soil moisture level within the same time period (with highest $r \approx 0.86$). However, once the primary effect of soil moisture for the concurrent period is removed, the residual inter-annual variability in NDVI is hypothesized to be able to highlight a memory effect from previous months or years. The objectives of this thesis is to identify and quantify such a memory effect between soil moisture and NDVI at sub-continental level, as well as to better describe the influence of land cover types as well as soil types on the identified memory effect. The data sets used in this study are as follows: (1) a 27-year NDVI time series from the Global Inventory Modelling and Mapping Studies (GIMMS) group, (2) a 27-year Modelled Soil Moisture data set provided by the Climate Prediction Centre (CPC) of the NOAA National Centres for Environmental Prediction (NCEP). (3) land cover map from Global Land Cover (GLC) 2000 and (4) Global Soil Regions map provided by the Natural Resources Conservation Service (NRCS) of United States Department of Agriculture (USDA).

Results indicate a 7-to-9 month time lags exist in western part of the Sahel (among countries i.e. Mauritania, Senegal, Mali, Guinea, and Ghana), as well as in the central to eastern parts of the Sahel (among countries i.e. Niger, Chad, Cameroon, Central African Republic, and Sudan). Other results have shown land covers with crops and open grassland with sparse shrubs are more sensitive to soil moisture changes than shrubs. Soil types with high water-holding capacities, such as Alfisols and Vertisols, if present in the environment, will ensure that shallow-rooted plants (i.e. Crops and grasses) will be intolerant to low soil moisture content 7-to-9 previous, especially in the dry years.

Keywords: Memory effect, Soil Moisture, Sahel, Rainfall, Land Cover, Soil Type, Remote Sensing

Acknowledgements

I would like to thank my supervisor Ass.Professor Jonathan Seaquist for his advice, support and encouragement on my work, and Mohamed Ahmed for providing the original data. I would also want to thank my dearest friend here in Lund for their invaluable friendships, Mohamed Ahmed, Minyi Pan, Mozarfar, Zeina Bali, Canzu, Vlad, Cole, Soheila, etc. Mostly, I would like to thank my parents for their unconditional love!

Table of Contents

Content

List of Figures and Tables

List of Figures

List of Tables

Chapter 1. Introduction

The Sahel has become the focus of much study over the last four decades mainly due to its vulnerability to drought as well as its sensitivity to climate change. The normalized difference vegetation index (NDVI) from NOAA Advanced Very High Resolution Radiometer (NOAA-AVHRR) has been used to determine the land surface response to precipitation variability (Anyamba & Tucker, 2005). According to several studies (Martiny et al., 2005; Philippon et al., 2005; Richard et al., 2008), evidence for a so called "memory effect" exists in different semi-arid African regions. It is defined as the persistence effect of rainfalls or soil moisture in vegetation dynamics.

The Sahel is the eco-climatic and biogeographic zone of transition between the Sahara desert in the North and Sudanian Savannas in the south. Countries lying within this region are always among the poorest, suffering from food insecurity, poverty and malnutrition (Food and Agriculture Organization of the United Nations [FAO], 2013). Nevertheless, the Sahel's population is growing at a rate of 2.6% per year, more than twice the global rate ("Climate Extremes", 2010), thus imposing more severe social-economic issues to the region.

In arid or semi-arid areas, vegetation growth is limited by rainfall (Richard et al, 2012). Less rain means less vegetation, and therefore less water to be recycled back to the atmosphere. This could explain the variation of precipitation at monthly, annual, and decadal time scales in places such as the West African Sahel (Los et al, 2006). Moreover, spring soil-vegetation water content anomalies found in Guinea strengthened the meridional gradient of soil-vegetation water content over the subcontinent, and were thought to contribute to the gradient of entropy which drives the West African monsoon (Philippon et al, 2005).

Therefore, studying the relationship, especially the memory effect, between soil moisture and vegetation greenness index, such as NDVI, can help in discovering the underlying processes which might be useful in explaining precipitation variation or climate change i.e. the change of West African monsoon in the Sahel region. Therefore, to help better understanding vegetation change in the region, it might be useful for early warning systems or future predictions.

1.1 Aims and Objectives

The overall aim of this thesis is to investigate if memory effect between soil moisture and NDVI exist at monthly or yearly time scales in Sahel at a sub-continental level.

1.2 Research Questions

I. Can memory effect be identified by using soil moisture and vegetation index data?
II. If the memory effect exists, what kind of land cover types and soil types does the memory effect associate with?

1.3 Thesis Outline

This paper is composed of 6 chapters. The first chapter is a brief introduction of the aims and objectives, as well as the structure of this paper. The second chapter talks about background of the study area. Description of materials and methods are covered in the third chapter. Results are displayed in chapter four, following with a discussion of the results in chapter five. Last but not least, a wrap up of the paper is summarized in chapter six.

Chapter 2. Background and Literature Review

2.1 Study Area

The Arabic word sāhil ساحل literally means "shore", describing the appearance of the vegetation of the Sahel as a coastline delimiting the sand of the Sahara. It is the ecoclimatic and biogeographic zone of transition between the Sahara desert in the North and Sudanian Savannahs in the south. It lies within a belt-shaped area which stretches from the Atlantic Ocean on the west to the Red Sea on the east. In terms of latitude and longitude, it is within the bounding coordinates of 10°N to 20°N in latitude and 15°W to 50°E in longitude. However, such boundaries cannot be determined explicitly, due to the fact that the precipitation or vegetation amounts that are used to delimit the boundaries are subject to large inter-annual and decadal fluctuations (Bader and Latif, 2003). In this paper, the study area is extended beyond the Sahel region, also including regions on the south along the Gulf of Guinea. Explicit information can be found in Figure (1) (Ahmed, 2012).

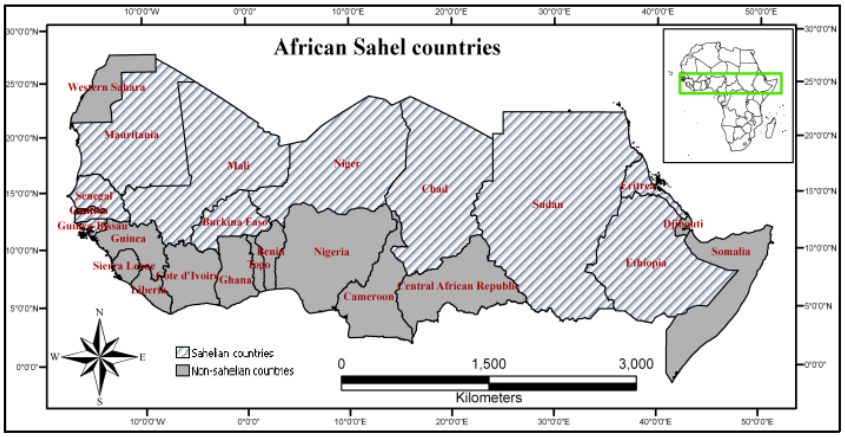

Figure 1. Overview of the geographic boundaries of the Study area and Sahelian countries. Reprinted from Ahmed, 2012.With Permission of the author.

Figure (1) shows the countries that belong to the Sahel. They have similar climatic conditions as well as cultural and livelihood systems (FAO/GIEWS, 1998). Approximately 50 million people were predicted to inhabit the region in 2000 (Mulford, 2008).

According to the "Sahel Weather and Crop Situation Report" conducted by FAO, the study area outlined in Figure (1) can also be

delimited to four different eco-climatic zones based on the average annual precipitation and agricultural features (FAO/GIEWS, 2007).
They are listed as below:
Sahelian zone: average annual precipitation ranges between 250 and 500 mm.
Sudano-Sahelian zones: average annual precipitation ranges from 500 to 900 mm.
Sudanian zone: average annual precipitation ranges from 900 to 1100 mm.
Guinean zone: average annual precipitation exceeds 1100 mm.

2.1.1 Climate in Sahel

Climate in the Sahel has shown variability for thousands of years at both inter-annual and inter-decadal time scales (Klönne, 2012).

Climate also varies by latitude. At the Sahel-Sahara border where latitude lies in 20°N, it is dominated by dry climate of the Sahara, whereas in the southern part of Sahel at 10°N, the climate is under the control of humid tropics (Hoerling et al., 2006). Thus, these two extreme climates lead to a strong meridional North-South rainfall gradient, with 100-200mm/year on the northern Sahel and 400-600 mm/year on the southern Sahel. The rainy season starts from June or July and extends to September. It peaks in August, with the rest of year experiencing dry conditions (Herrmann et al., 2005). It is claimed that approximately 83% of the annual rainfall falls between July and October in the Sahel (Lamb, 1980). Such an annual cycle is driven by the meridional displacement of the Inter-tropical Convergence Zone (ITCZ). On land, the ITCZ moves back and forth across the Equator following the Sun's zenith point. Therefore, when solar insolation reaches its maximum in the northern hemisphere, the ITCZ moves to the northernmost position in the boreal summer and provides the Sahel with rain. Similarly, when it moves to the southern hemisphere during the austral summer, climate in Sahel becomes dry and is influenced by the subtropical high pressure belt (Klönne, 2012). The ITCZ arrives first in April at 5°N and stays at this quasi-stable position until the end of June, thus bringing the first Guinean rainy season. Then, the ITCZ quickly shifts during the first half of July to 10°N and stays at this second quasi-stable position till the end of August. (Philipphon et al, 2005). Up until this time, rainfall is fully developed at the Sudano-Sahelian region, leaving the Guinean zone with the lowest precipitation. Lastly, the ITCZ progressively withdraws from its northernmost position between September to November which leaves

the Sudanian and Sahelian bands with low precipitation as the precipitation moves once over Guinea.

Besides the ITCZ, other factors which cause the fluctuation of precipitation in the study area are the African Easterly jet (AEJ) and Tropical Easterly Jet (TEJ). Both their position and intensity play a significant role in precipitation fluctuations (Paeth and Hense, 2004). The AEJ has similar movement in time with respect to other atmospheric systems such as the ITCZ (Klönne, 2012).

Moisture supply in the Sahel can be divided into three parts. The first moisture source for the land is from the adjacent oceans, particularly the tropical southern Atlantic. Moreover, the strongest flow from the ocean to the land happens along the coast of Guinea, which is the most important source of moisture for the Sahel (Hagos and Cook, 2008). The second part of the moisture supply is the evaporation from the land surface, and it contributes to one third of the total moisture supply (Giannini et al., 2003). The third part comes in particularly in the summer and it is influenced by the low-level West African monsoon, which is formed due to the strong land-ocean contrast, thus causing moist air from the ocean lowing into the continent from the southwest, and causing precipitation events (Hagos and Cook, 2008).

2.1.2 Rainfall in Sahel

In the 20th century, rainfall variability appeared to be dominated by variations on an inter-annual scale until the 1950s (Klönne, 2012), when there was a shift in variability to the inter-decadal time scale (Hulme et al., 2001). From the 1950s to 1960s, precipitation amounts in the Sahel were highly relative to the 20th century mean (Brooks, 2006) and this trend had persisted over two decades.

After that, precipitation amounts decreased dramatically. The exact starting date and end date of the desiccation are hard to determine; the approximate time period is between late 1960s until the late 1980s or early 1990s (Hagos and Cook, 2008). In particular, the 1980s is estimated to have been the peak of the dry period (Paeth and Hense, 2004). According to the IPCC report, a rainfall decrease of 29-49% has been observed in the 1968-1997 period compared to the 1931-1960 baseline period within the Sahel region (IPCC, 2001). In particular, the lowest records of annual rainfall values in the history of the Sahel were in the year of 1983 and 1984, nevertheless, severe droughts also occurred in 1972, 1973, and 1977 (Hulme, 2001). The

drought of 1984 was very severe and affected all countries from Mauritania to Ethiopia, including several bordering countries on the southern edge of the Sahel. However, drought in 1973 was more localized which affected mostly Mali, Niger and Chad.

After the peak in low rainfall in the mid-1980s, precipitation values have started to rise again (Klönne, 2012). Rainfall variability also seemed to shift back to the inter-annual trend pattern from the inter-decadal trend pattern in the mid-1990s (Klönne, 2012). In particular, annual precipitation rates reached up to the 1961-1990 climatological mean in the central and eastern Sahel, however, parts of the western Sahel still remained dry (Klönne, 2012). Moreover, Giannini et al. (2008b) found that the intensity of the precipitation events has increased, a pattern consistent with what could be expected with global warming

2.1.3. Vegetation in Sahel

Vegetation and its dynamics, i.e. the changes in distribution, density and composition of species (Vanacker et al., 2005), can be observed in many ways, but one of the most effective ways is through remote sensing techniques. Vegetation indices such as the Normalized Difference Vegetation Index (NDVI) are most commonly used, and can be calculated from the remotely sensed satellite images. NDVI is defined as,

$$NDVI = \frac{QNIR - QRed}{QNIR + QRed} \quad (1)$$

Where QNIR is the reflectance in the Near-Infra Red (NIR) and QRED is the reflectance in Red band.

NDVI measures the photosynthetic activity and green biomass of healthy green leaves, because vegetation reflects NIR radiation due to its internal mesophyll structure and absorbs red radiations due to chlorophyll and other pigments (Tucker et al., 1985). Therefore, it is a good indicator for leaf area index (LAI) (Asrar et al., 1984) and Net Primary Production (NPP) (Nemani et al., 2003; Sjöström et al., 2009).

By using the above-mentioned products, it has been observed that vegetation cover decreased dramatically in the 1970s and 1980s (Klönne, 2012). Moreover, Sahelian species' richness declined by 14 ± 4% between 1945 and 1989 (Gonzalez, 2001). Starting from the early 1980s, satellite observations of the NDVI have revealed a start of re-greening in the Sahel (Seaquist et al., 2009, Hickler et al., 2005, Olsson et al., 2005, Herrmann et al., 2005).

Despite its inter-decadal variations, vegetation dynamics also have its annual patterns in the region of Sahel. It follows the similar patterns of rainfall, which developed at the highest level in August-September, and with the highest values recorded at the western and eastern extremes of the region (Anyamba & Tucker, 2005).

In terms of species, the Sahelian zone is characterized by very sparse vegetation cover of annual and perennial grasses with thorny shrubs interspersed in-between. Conversely, taller vegetation of woody species with high amount of ground cover dominates in the Sudanian and Guinean zones (Le Houerou, 1980).

2.2 Driving Forces of the Rainfall Variations in Sahel

Rainfall variability observed in the 20th century has far reaching influences on human welfare. Long lasting dry years will result in problems such as crop failure and livestock decline. On the contrary, wet years with erratic and stormy rainfall will also bring problems to the region, as floods can make people homeless and ruin their harvests. It has been reported that countries across the Sahel belt have suffered from the floods which does damage to crops, livestock and property.

It is therefore important to understand the mechanisms of the rainfall variation, thus make better predictions for future preparations.

2.2.1 20th century climatology

In terms of explaining the 20th century precipitation variability, three factors are thought to be equally dominant over the story. They are 1) anthropogenic causes; 2) external forcing: sea surface temperature changes; 3) internal mechanism: land surface-atmosphere feedbacks (Klönne, 2012).

2.2.1.1 Anthropogenic Causes

According to the theory of anthropogenic causes brought up by J.G. Charney in 1975, human mismanagement and overuse of the vegetation and the soil, such as the expansion of agricultural land, overgrazing and deforestation, can causes localized feedbacks between land surface conditions and atmospheric radiation (Hagos and Cook, 2008). As a consequence, the surface albedo will increase, which induces a reduction in surface heating and thus atmospheric heating. As a result, convection will be dampened as well as the scale of precipitation, thus vegetation covers will diminish which in return amplifying the initial change, and making it a positive feedback. This theory is famous as "Charney's hypothesis" (Giannini et al., 2008b).

Although this theory seems possible in explaining the reasons behind the 20th century drought, it is claimed by other researchers that the albedo changes have proven to be exaggerated (Nicholson et al., 1998).

2.2.1.2 External forcing: Sea Surface Temperature Changes

In the mid-1980s, a new theory came along and replaced the prevalent theory of anthropogenic causes. According to a recent climatic model constraint by only oceanic forcing, rainfall variability from July-September during the years 1930-2000 can well be matched with modelled values (Giannini et al., 2003). Moreover, by using five different climate models as well as conducting a total of 80 experiments, Hoerling et al. (2006) have been able to prove that rainfall spatial-temporal variability can be explained by global sea surface temperatures (SSTs).

The occurrence of drought in Sahel is due to a warming of the equatorial Indian Ocean as well as a differential heating of the tropical Atlantic, i.e. a warmer South than North Atlantic and a warming of the Pacific Ocean (Giannini et al., 2008b).The mechanisms underlying the SSTs can be summarized into two aspects. The first regards changes in the movement of the ITCZ. As the Indian and Atlantic Ocean warms up, the ITCZ tends to stay further to the south along with the warmer waters and will therefore not be able to provide the Sahel with the same amount of rainfall (Held et al., 2005). The second factor causing the influence of the oceanic forcing is the transport of moisture into the Sahel. When the ocean warms, land-ocean temperature contrast is weakened and evaporation from the ocean surface increases (Hagos and Cook, 2008). These mechanisms will indirectly change the divergent and convergent motions over the continent as well as oceans, thus depriving the Sahel of its moisture. This accounts for a moisture loss of about 50% from the Sahel region across the West African coast (Hagos and Cook, 2008).

2.2.1.3 Internal Mechanism: Land Surface-Atmosphere Feedbacks

Besides the external forcing of changing SSTs as the key driver for Sahelian wet and dry periods, the land surface's interactions with atmosphere as a response to the external climatic forcing is said to have a significant role in controlling the rainfall anomalies on a regional or local scale (Zeng et al., 1999; Giannini et al., 2008b). Such interactions are known as feedback mechanisms, and are defined as responses of the climate system to an external forcing, which leads to amplify or dampen the initial change-a positive or a negative feedback (Hansen et al., 1984). There are two feedback

mechanisms mostly relevant to the Sahel climate change, which are vegetation and dust (Klönne, 2012).

Vegetation feedback can be identified through changes in evapotranspiration and surface albedo (Klönne, 2012). For example, vegetation will influence on the local moisture availability directly through evapotranspiration and indirectly through modifying the soil moisture content and thus the evaporation from the soil. Studies have suggested that vegetation loss in the Sahel accounts for about 10% of the observed decline in precipitation (Yoshioka et al., 2007). Moreover, deforestation in the West African coast region is found to cause the decline of regional rainfall, due to the collapse of the monsoon system. Therefore, the western Sahel is suspected to be the region where the vegetation-atmosphere feedback is strongest (Brooks, 2004).

On the other hand, the feedback effect from dust can either enhance the precipitation amount or dampen it. It depends on its interaction with the atmosphere, because dust could prevent incoming solar radiation from reaching to the Earth surface through reflection and scattering, thus causing a cooling effect to the Earth's surface, or it could reduce the amount of long wave radiation from leaving the Earth's surface through absorption, therefore leading to a warming effect. However, which one of these effects may dominate is still unknown.

2.2.2 21st century climatology

Different climate models may produce different results as they integrate different drivers of climate variability. Thus, predictions for future climate in Sahel call for either wet or dry conditions. For a wetter Sahel, conclusions are drawn that global warming would cause the land-ocean temperature contrast to increase, thus result in increasing precipitation in the Sahel (Giannini et al., 2008a; Maynard et al., 2002). Therefore, the Sahel may benefit from the effects of anthropogenic climate change (Klönne, 2012). For future drying predictions, they are associated with the warming of the southern Atlantic and equatorial Indian Ocean, and can be explained by the reduced land-ocean temperature gradient. However, the likelihood of such a trend is still unknown and some researchers such as Cook and Vizy (2006) argue that the wetting of the region due to increasing moisture inflow from the ocean is more likely to happen, and it would require a warming of 3°C of the SST of the Gulf of Guinea.

2.2.3 Literature Review

Studies focusing on finding the lagged relationship between rainfall data and NDVI or soil moisture data and NDVI can be summarized into two groups. One with focus on intra-annual memory effects, and the other with focus on inter-annual memory effects.

Studies that focus on identifying the intra-annual memory effects are summarized below. One such study is conducted in Kansas, US. It contains three climatic types, according to the Köppen climate classification, which is humid continental, semi-arid steppe, and humid subtropical, respectively. By calculating the correlation coefficients between bi-weekly NDVI and precipitation data, results had shown that NDVI responded to a major precipitation event after 2-4 weeks (Wang et al., 2003). Another study conducted in the semi-arid region of south-western USA was based on investigating the lagged effect between vegetation index (NDVI and EVI) and in-situ measured soil moisture. Correlations were calculated by using raw time series of NDVI and soil moisture with daily temporal resolutions. Results had revealed that the vegetation index had the highest correlation with soil moisture at 5-to-10 day time lags (Schnur et al., 2010). Other studies involving the intra-annual memory effects include from Nicholson et al. (1990), the results have shown that NDVI correlates well with precipitation amounts in the concurrent plus 1 to 2 previous months; Justice et al. (1991), using 10-day composites, find out vegetation response time to rainfall is 10 to 20 days.

Regarding inter-annual memory effects, Philippon et al (2005) adopted three time series data (from 1991 to 2000), which are NDVI, soil-vegetation water content (sigma_0) and precipitation (PPT) data, to conduct either serial correlations or cross correlations among the data sets. Sigma_0, refers to the backscattering coefficient, and is a measurement of vegetation and soil water content. It is a remotely sensed product comes from the Scatterometer instrument (WSC) on board the European Remote Sensing satellite (ERS). Serial correlation is the correlation between one time series data and itself at different time lags. Cross correlation is the correlation between two different time series data. Thus, the result has shown that NDVI or sigma_0 anomalies observed in September to October have significant correlation coefficients with those observed 7 to 9 months later in April to June in the West Sahel. Another result of this study has clearly pointed out a memory effect between sigma_0 and precipitation data. Specifically, sigma_0 anomalies in spring at Guinea region can be explained by precipitation anomalies in the previous autumn. This pattern is thought to be an indirect driver of

the West African monsoon through its positive effect which strengthens the meridional gradient of soil-vegetation water content over the sub-continent. Moreover, Martiny et al. (2005) has also found out a relationship between annual NDVI and annual PPT time series in the South Sahel. By applying multiple-regression models, results have shown annual NDVI values can be explained better if concurrent year as well as previous year PPT data was used in the model. Last but not least, the studies conducted by Richard et al. in 2008 and 2012, have discovered two memory effects by adopting a different approach compare to the ones mentioned previously. Instead of studying the relationship between soil moisture and NDVI at different lag periods, Richard et al. (2008) have used residual time series calculated from simple linear regression model between soil moisture and NDVI at the "early summer", to regress it with different predictors, such as rainfall amounts, number of rainy days, rainfall intensity, etc., thus to identify the memory effect by choosing the time lag period where a predictor shows high correlation values with the residuals. Accordingly, the author named these two memory effects as mem1 and mem2. Memory 1 effect is dominated by NDVI average in early raining season and is becoming effective after one year, thus, having a positive correlation with NDVI values the following year; Memory 2 effect is dominated by Rainfall in late raining season, and lasts over a 7-10 month period, which, as a result, do not support the green-up of the next early summer. In a later study published in 2012, they have further related these two memory effects with the land cover and soil types, in order to better describe the influence of soil and vegetation characteristics on these two memory effects. Results have indicated that open grassland comprising an herbaceous layer growing on Aerosols is the most sensitive vegetation type to mem1, and mem2 has significant negative correlations with all the vegetation and soil types.

Chapter 3. Materials

3.1. Datasets

A set of remotely-sensed NDVI time series data as well as modelled soil moisture time series data set, both spanning from 1982 to 2008 are used in this thesis. In addition, a land cover map as well as a soil texture map is used. They are described in detail as below.

3.1.1. GIMMS NDVI Data Sets

The Global Inventory Modelling and Mapping Studies (GIMMS) normalized difference vegetation index (NDVI) data sets were generated to provide a 1981+ satellite record of monthly changes in terrestrial vegetation. The data sets are derived from the AVHRR instrument on-board of National Oceanic and Atmospheric Administration (NOAA) polar orbiting satellite series 7, 9, 11, 14, 16 and 17. The AVHRR has five different spectral bands at 1.1 km spatial resolution, one in the visible, one infrared and three thermal bands. GIMMS data use the first and second band. Notice that except for the downloadable 25 years of data, data in 2007 and 2008 are provided from Eklundh, L. after contacting the data provider.

This NDVI datasets have been adjusted by the GIMMS group at NASA's Goddard Space Flight Centre. Correction of inaccuracies involved with lacking of on-board band calibration, atmospheric effects, variation in solar illumination, volcanic aerosols, effects of satellite drift and sensor view angles have been carried out. Moreover, two 15-day composites were constructed by choosing pixels with the maximum values during regularly spaced intervals, thus to minimize the effects of water vapour and cloud cover that strongly reduce NDVI values (GIMMS data documentation).

The GIMMS NDVI data of two 15-day composite were further adjusted by Ahmed (2012) into monthly data set, the method he used is the same as the GIMMS group which is choosing pixels with maximum NDVI values from the two images, and combines them into one. Thus, the data set adopted from this study was monthly NDVI with maximum value composites (MVC) at an 8 km spatial resolution.

To evaluate the quality of GIMMS NDVI data, Fensholt et al., (2006) used NDVI from SPOT-4 VGT data as comparison to GIMMS NDVI data, because the former had better sensor design and data processing, therefore was considered as an improvement over

AVHRR. Results had shown a match between AVHRR GIMMS NDVI and SPOT-4 VGT NDVI at 8km resolution between 1998 and 2004. Furthermore, Ortho-regression analysis between annually integrated values of AVHRR GIMMS NDVI and SPOT-4 VGT NDVI had shown high correlations between the two. Therefore, it is concluded by the author that the AVHRR GIMMS NDVI is consistent with SPOT-4 VGT NDVI, and can be considered as accurate (Fensholt et al., 2006).

For more information about GIMMS NDVI data set or for downloading the product, please go to: (http://glcf.umiacs.umd.edu/data/gimms/) [Data accessed in April, 2012].

3.1.2. Modelled Soil Moisture Data

The Modelled soil moisture data sets covering the period of 1982-2008 were adopted in this study. It covers the same period compared to the GIMMS NDVI data set. This modelled soil moisture data set was provided by the Climate Prediction Centre (CPC) of the NOAA National Centres for Environmental Predictions (NCEP). As a result, 0.5°x 0.5° monthly global soil moisture data sets for the period from 1948 to the present were produced. The land model used is a "bucket" water balance model, and the associated inputs are Climate Prediction Centre monthly global precipitation over land, which uses over 17,000 gauges worldwide, and monthly global temperature from a global reanalysis, whereas outputs consists of global monthly soil moisture, evaporation, and runoff, starting from January 1948.

An outstanding feature of this data set is that all fields are updated monthly. Moreover, model validation by using observed soil moisture measurements in different places around the word, i.e. China, Russia, India and USA, have shown that the modelled soil moisture simulates the seasonal to inter-annual variability of observed soil moisture very well (Fan and Huug van den Dool, 2004). A study of the NASA/DLR satellite mission GRACE had shown that monthly GRACE gravity field can be used to recover monthly changes in water storage (Wahr et al., 2004). Early results of GRACE for 2002 and 2003 had shown remarkable similarity between the modelled soil moisture annual cycle and information captured by GRACE (Fan and van den Dool, 2004).

The model had set the effective water holding capacity to 76cm of water, which at a porosity of 0.47 corresponds to a 1.6-m-deep "leaky" bucket (Fan and Huug van den Dool, 2004). The maximum soil moisture value was set to 760mm in the model, and output units for soil moisture data were in millimetres.

For more information about the modelled soil moisture data set or for downloading purposes, please go to: (http://www.cpc.ncep.noaa.gov/soilmst/leaky_glb.htm)[Data accessed in April, 2012].

Table 1. Summary of characteristics of GIMMS NDVI and modeled soil moisture data. Reprinted from Ahmed, 2012. With Ahmed's Permission.

Datasets	Spatial resolution	Spatial extent	Temporal resolution	Temporal extent	Availability and cost	Limitations
GIMMS NDVI datasets	8 km* 8km	Global	Monthly	1981 to 2008	Available online and free	In highly dense vegetation areas, NDVI has a lower accuracy.
CPC - GMSM	0.5° * 0.5°	Global	Monthly	1948 to present	Available online and free	Maximum soil moisture is 760 mm and the great modelled depth (=1.6 m)

3.1.3 Land Cover Data

The Global Land Cover (GLC) 2000 map is used in this study. It is constructed based on observations made by the VEGETATION sensor on the SPOT 4 satellite from 1st November 1999 to 31st December 2000. Its objective was to provide a harmonized land cover database over the whole globe for the year 2000 The GLC 2000 was mainly produced by unsupervised classification aided by thematic maps and class spectral statistics.

In this study, the GLC 2000 map was clipped to the study region from its Africa origin, and then the newly clipped map was resampled to 8km from 1km spatial resolution by using the nearest neighbour interpolation method. Moreover, the map has a legend with 27 classes which were based on the FAO LCCS (land cover classification system) (Mayaux et al., 2006).

The accuracy assessment conducted by Mayaux et al. (2006) had indicated an accuracy of 68.6%.

For more information about GLC 2000 Land cover data or for downloading purposes, please go to: (http://bioval.jrc.ec.europa.eu/products/glc2000/glc2000.php) [Data accessed in August, 2012].

3.1.4. Soil Texture Data

The Global Soil Regions map provided by the Natural Resources Conservation Service (NRCS) of United States Department of Agriculture (USDA) is adopted in this study. This map is based on a reclassification of the FAO-UNESCO Soil Map of the World combined with a soil climate map of USDA-NRCS. It is classed by Soil Taxonomy Suborders of 99 classes, which can also be regrouped into 12 soil orders according to Soil Taxonomy. It has a global coverage, in geographic projection, with minimum scale of 1:5,000,000. The data is first produced on April, 1997 and revised on September, 2005.

In this study, the Global Soil Regions map was clipped to the study region, and resampled to 8km spatial resolution using nearest neighbour interpolation method. Soil suborder classes were merged to the 12 soil orders according to USA Soil Taxonomy.

The data provider has not described the quality of this data; however, the soil map adopted in this study is converted from the FAO Soil Map of the World, and soil climate map. Thus a conversion will require assigning suborder to every combination of FAO classification and soil climate map. Nevertheless, direct correlations are not always available for such a conversion, therefore might impose uncertainties for certain area or class.

Information about the soil taxonomy can be found at: (http://soils.usda.gov/technical/classification/taxonomy/)[Data accessed in March, 2013].

Descriptions of the characteristics of the 12 soil orders together with their percentage and location in the world can be found in table 2.

For more information about the Global Soil Regions map or for downloading purposes, please go to: (http://soils.usda.gov/use/worldsoils/mapindex/order.html)[Data accessed in August, 2012].

Table 2. Characteristics of the major 12 soil order classes summarized according to USDA-NRCS website. Reprinted from Ahmed, 2012 and Revised in June, 2013. With Ahmed's Permission.

Soil order	Location	Description	Soil Texture	Area (%) in the world
Alfisols	Semiarid to moist areas	Characterized by holding water and nutrients to plants, occurs under high dense vegetation regions like as forest or mixed vegetation cover and it's a good productive soil for crops.	clayey (water is held at less than 1500 kPa tension during at least 3 months each year when the soils are warm enough for plants to grow)	10%
Andisols	Cool areas with moderate to high precipitation	High water and nutrient-holding capacity associated with volcanic materials and tend to be highly productive soils.	loam (high water- and nutrient-holding capacity, contains minerals and ashes from volcanic activities)	1%
Aridisols	Deserts of the world	Highly dry soil for the growth of plants, characterized by lack of moisture and accumulating gypsum, and salt.	stony (too dry for the growth of plants)	12%
Entisols	Occur in many environments	Characterized by absence of pedogenic horizon development and likely to found in flood plains, dunes and steep slopes.	fine sandy and clayey	16%
Gelisols	Common in higher latitudes or at high elevations	Characterized by a permafrost or ice aggregation near the soil surface.	N/A	9%
Histosols	Occur in highly saturated areas all the year round	Have a high content of organic matter and no permafrost and commonly called bogs, peats or mucks.	N/A	1%
Inceptisols	Semiarid to humid environments	Characterized by a moderate degree of soil weathering and development in a wide variety of climates.	fine sand	17%
Mollisols	Occurs on the steppes of many countries.	Characterized by moderate to high moisture deficiency and high content of organic matter. Usually occurs under grass.	clayey (high in content of organic matter, formed under grass in climates that have a moderate to pronounced seasonal moisture deficit)	7%
Oxisols	Tropical and Subtropical regions	Characterized by low fertility and a low capacity to retain additions of lime and fertilizer.	fine sandy (high permeability, and resistant to compaction)	8%
Spodosols	Under coniferous forests of humid regions	Occur in areas of coarse-textured deposits and it tends to be acid and infertile.	sandy	4%
Ultisols	Humid areas	Nutrients are concentrated in the upper zone of soil, and it is classified as acid soils that can't retain addition fertilizer and lime easily.	clayey (acid soils in which most nutrients are concentrated in the upper few inches)	8%
Vertisols	Occur in many environments	Characterized by high content of expanding clay minerals that transmit water very slowly and tend to be high in natural fertility.	clayey (transmit water very slowly and have undergone little leaching)	2%

3.2 Methodology

The method adopted in this study is based on a study by Richard et al in 2008. Instead of using rainfall data, soil moisture data was adopted. More specifically, the method applies linear regressions which relate NDVI and soil moisture data sets. NDVI residuals, which cannot be explained by soil moisture data in the concurrent period, is again linearly regressed with soil moisture data calculated from four tri-monthly periods with different yearly time lags, thus to investigate the existence of a memory effect.

3.2.1 Data Pre-processing

At first, both of the GIMMS NDVI data set as well as the SM data set were clipped to the study area domain, which is from 5°N to 20°N in latitude, and 20°W to 55°E in longitude.

When downloaded from the Global Land Cover Facility website, the GIMMS NDVI data set was scaled to values ranging from -1000 to 1000. To recover the NDVI range of -1 to 1, the raw data set was divided by 10000. Last, the GIMMS NDVI data set was projected using nearest neighbour to Albers Equal Area Conic projection by using Clarke 1866 ellipsoid.

The soil moisture (SM) data set was first of all re-projected to Albers Conical Equal Area Projection using the nearest neighbour interpolation algorithm. In order to have the same spatial resolution as the NDVI data set, the re-projected SM data sets were then resampled from 0.5° to 8km. The method used in resampling is the nearest neighbour algorithm. Notice, that method only assign values to the cells in an output raster according to the nearest cell in an input raster, therefore it does not change any of the values of cells from the input layer.

In arid or semi-arid areas, vegetation greenness difference is influenced by the amount of precipitation (Richard et al., 2012). A time interval is determined by what is known as ecosystem functioning, which depicts vegetation dynamics between the last month of the dry season and the start of the rainy season (Richard et al, 2012). Therefore, the greenness difference over the study area is estimated from the difference between the NDVI in April, i.e. the start of the raining season in Guinean zone, and the NDVI in August, i.e. maximum rainfalls in Sudano-Sahelian zone and minimum rainfalls in Guinean zone. This difference is thereafter denoted $NDVI_{Aug-Apr}$. Such a greenness difference is calculated by subtracting NDVI values in

April by NDVI values in August of each year, and a new $NDVI_{Aug-Apr}$ time series date set is hereafter produced. The same operations were applied to the SM data set too, and hereafter named $SM_{Aug-Apr}$. The purpose of retrieving such two yearly time series of NDVI and SM were to calculate the residual time series from the linear regression, in order to retrieve the NDVI variations which could not be interpreted as direct vegetation responses to soil moisture during the concurrent time period.

Besides retrieving annual SM values over the vegetation greenness difference period, soil moisture content within a three-month period was also calculated at different time lags by using the same method as before. For example, soil moisture content time series between October and December with a one-year time lag is calculated by subtracting SM values in October from SM values in December at each year from 1982 to 2007. It is named shortly as SM (12-10) _1. Moreover, SM (12-10) _2 means same tri-monthly period between October and December with a two-year shift in its time series (1982-2006). Additionally, 29 of such soil moisture tri-monthly time series were produced, and they represented soil moisture content over each tri-monthly period with yearly time lags up to seven years. They can be found in order in table (3).

Thus, two new data sets both containing values between April and August of each year as well as 29 SM tri-monthly time series with time lags are produced, and were ready to be used in further linear regression analysis for the purpose of determining the memory effect.

Table 3. Independent versus (vs.) dependent variables with time series periods shown for each.

Time Lags (in Years)	Independent Variable	Time Series Period	Linear Regression	Dependent Variable	Time Series Period
Lag 0	SM(3-1)	1982-2008	vs.	Residuals	1982-2008
Lag 1	SM(12-10)_1	1982-2007	vs.	Residuals	1983-2008
	SM(9-7)_1				
	SM(6-4)_1				
	SM(3-1)_1				
Lag 2	SM(12-10)_2	1982-2006	vs.	Residuals	1984-2008
	SM(9-7)_2				
	SM(6-4)_2				
	SM(3-1)_2				
Lag 3	SM(12-10)_3	1982-2005	vs.	Residuals	1985-2008
	SM(9-7)_3				
	SM(6-4)_3				
	SM(3-1)_3				
Lag 4	SM(12-10)_4	1982-2004	vs.	Residuals	1986-2008
	SM(9-7)_4				
	SM(6-4)_4				
	SM(3-1)_4				
Lag 5	SM(12-10)_5	1982-2003	vs.	Residuals	1987-2008
	SM(9-7)_5				
	SM(6-4)_5				
	SM(3-1)_5				
Lag 6	SM(12-10)_6	1982-2002	vs.	Residuals	1988-2008
	SM(9-7)_6				
	SM(6-4)_6				
	SM(3-1)_6				
Lag 7	SM(12-10)_7	1982-2001	vs.	Residuals	1989-2008
	SM(9-7)_7				
	SM(6-4)_7				
	SM(3-1)_7				

3.2.2 Regression Analysis Set-Up

The aim of this study is to investigate if a memory effect can be identified by SM and NDVI data in Sahel at a sub-continental level. In the first step, simple linear regression models were calculated between $NDVI_{Aug\text{-}Apr}$ and $SM_{Aug\text{-}Apr}$ time series and as a result, a time series of residuals were produced. In the second step, simple linear regression models were again used between the residual time series produced in the previous step and the corresponding SM time series at different pre-processed time lags. Table (3) lists out both the variables as well as the associated time period of each time series.

3.2.3 Simple Linear Regression Analysis

While correlation analysis is used to measure the strength of the linear association between variables, regression analysis is about studying the relationship between a dependent variable and a set of independent explanatory variables. If the modelled relationship is valid, one can later on use the independent variable to predict the values for the corresponding dependent variable, though with some degree of uncertainty. Thus, in the first step of linear regression analysis of this study, $SM_{Aug\text{-}Apr}$ was the independent variable which explains the dependent variable of $NDVI_{Aug\text{-}Apr}$. In the second step, the residual time series is explained by soil moisture content over different tri-monthly period at seven lag years, respectively.

As the final products from the linear regressions, a set of residual time series, an image showing Pearson's correlation coefficients (r values), and an image showing coefficient of determination (R^2 values) were produced and used in the analysis. Notice, both the meaning of r and R^2 will be explained in the latter part of this chapter.

3.2.4 Checking Statistical Assumptions

As linear regression analysis is mainly used in this study, it is important to check the data sets used within the analysis violate any underlying statistical assumption.

$NDVI_{Aug\text{-}Apr}$ and $SM_{Aug\text{-}Apr}$ yearly time series are used for inspection purposes; because they are the data sets will be used in the regression analysis, not the monthly time series.

The following statistical tests are used to check for violation of assumptions in the original data sets. The results are presented in Chapter 4.

Breusch-Pagan test (named after Trevor Breusch and Adrian Pagan) is used to test for heteroscedasticity in the linear regression model. If the variances of the residuals calculated from the fitted model are equal (homoscedasticity), then they do not depend on the independent variables. Thus, a simple linear model can be set up by regressing the squared residuals on the independent variables, using a regression equation of the form,

$$\hat{u}^2 = \gamma_0 + \gamma_1 x + v. \quad (2)$$

Where $\hat{u}^2$ is the average of the squared values, x is the independent variable, v is the error terms.

The null hypothesis is homoscedasticity, and the test used for such a hypothesis is the F-test, if the test result confirms that the independent variables are jointly significant then the null hypothesis of homoscedasticity can be rejected. R is used to perform the Breusch-Pagan test on 19 randomly selected sample points extending across the entire study area.

Durbin Waston test detects the first order autocorrelation present in the residuals from a regression analysis. The equation for the Durbin Waston statistic (d) is:

$$d = \frac{\sum_{t=2}^{T}(e_t - e_{t-1})^2}{\sum_{t=1}^{T} e_t^2}, \quad (3)$$

Where e_t is the residual value at time t.

Its value always lies between 0 and 4. A value of 2 indicates no serial autocorrelation. A Durbin-Watson statistic less than 2 indicates evidence of a positive serial correlation and statistic greater than 2 indicates evidence of a negative serial autocorrelation.

3.2.5 Memory Effect Determination

In order to find out the time lag period when a memory effect may occur, R^2 calculated from the linear regression model between residuals and soil moisture content with time lags is compared. The average R^2 with highest value is considered as the potential candidate for a memory effect. R^2, sometimes called the coefficient of determination, can be defined as the proportion of the total variability in y explained by the regression, and it is equal to the square of the correlation coefficient.

Pearson's correlation coefficient (r), which can be explained as a measurement of the strength of the linear association between variables,

$$r = \frac{\mathrm{COV}(X_1,\ X_2)}{S1\ S2} = \frac{\sum_{i=1}^{n}[(X_{1i} - \bar{x}_1)\,(X_{2i} - \bar{x}_2)]}{(n-1)S1S2} \quad (4)$$

Where X_{1i} and X_{2i} are the sample observations of the two variables; $\bar{x}_1$ and $\bar{x}_2$ refer to the sample means; S_x and S_y are the sample standard deviations of variable X_1 and X_2, respectively.

To determine whether r is significant, one can apply student's t-test, which follows a Student's t distribution if the null hypothesis is supported. Thus, the null hypothesis is stated as the true correlation coefficient, ρ, is equal to zero. The test is carried out by forming the t-statistic:

$$t = \frac{r\sqrt{n-2}}{\sqrt{1-r^2}} \quad (5)$$

Whereas, n is the sample size, and r is the correlation coefficient. As a result, the minimum absolute value of r required for significant with different n are displayed in table 6 of Chapter 4.

3.2.6 Memory Effect Stratification

After finding out the time of when the memory effect happens every year, it is more important to look into this effect and understand its mechanisms.

Instead of using the overall residual time series produced from the linear regression model of soil moisture and NDVI over the growing season, the residual time series was divided into two categories, one with positive values and the other one with negative values. The positive residual time series can be interpreted as above-normal NDVI values, and the negative one can be interpreted as below-normal NDVI values. Due to the influence of the memory effect, these anomalies can then be explained by soil moisture content in a linear model. Spatial locations with significant R^2 values are thereafter displayed in maps.

Besides the investigation of the memory effect via NDVI anomalies, it is also interesting to look into the characteristic of each cluster formed under the memory effect, therefore to investigate the residual and soil moisture content relationships at specific locations rather than the entire study area. In order to do this, a 3 by 3 kernel were used to extract average information from each correlation between residuals and soil moisture content with time lags, at the locations where clusters are in dominant and the memory effects are particularly strong. Thus, 14 and 15 sample points were taken from the images that show a memory effect with positive residuals and memory effect with negative residuals, respectively.

Moreover, if r has a positive value, it represents a positive relationship between the two variables, and vice versa. Therefore, r is assessed after differentiating between above-normal and below-normal NDVI anomalies. For the convenience of differentiation, they are hereafter grouped into four scenarios: (1) above-normal mem7-9 with positive significant r values; (2) above-normal mem7-9 with negative significant r values; (3) below-normal mem7-9 with positive significant r values; (4) below-normal mem7-9 with negative significant r values. Thus, to measure out the positive or negative relationships between soil moisture and NDVI residuals, and to

associate them with land cover types as well as soil types. As a result, the implication of memory effects can be explained by soil and vegetation according to their characteristics.

3.2.7 Land Cover and Soil Type Association with the Memory Effect

After knowing the implications of the memory effects of NDVI anomalies with respect to positive and negative significant r values, it is worthwhile to investigate their associations with environmental factors such as land cover and soil texture type In order to shed some light on what may lie behind the patterns.

The raster image with significant positive and negative r values which represent the four scenarios are first of all overlaid with the Global land cover 2000 map, then the overlaid raster images were intersected with the soil texture map. As the attribute tables from both images are joined, one can find out the soil types for each land cover types overlaid with memory effects found in the four scenarios. Such results can be found in table 16, 17, 18, 19, 20 and 21 of Chapter 4.

Chapter 4. Results

4.1 Data Sets Selected

The Original GIMMS NDVI Data and Modelled Soil Moisture Data were tested according to the linear regression assumption rules.

4.1.1 Checking for linear regression assumptions

The first linear assumption is stated as,
The relationship between y and x is linear; that is, there is an equation, $y=\alpha+\beta x+ \varepsilon$ that constitutes the population model

In one of the hypotheses, the assumption is that a linear relationship exists between NDVI and Soil Moisture. NDVI values within the greenness period of each year were the dependent variable while Soil Moisture values within the same greenness period of each year were the dependent variable. After running the models for the original datasets, the following r image is generated in Figure (2) and the associate statistics are listed in table (4).

Table 4. Linear regression results for the original data sets.

Data Sets	Number of time series images (n)	Minimum r value	Maximum r value	Significant level of r (using t-test two tailed, α =0.05)
Original Datasets	n= 27	-0.70	0.86	-0.381; 0.381

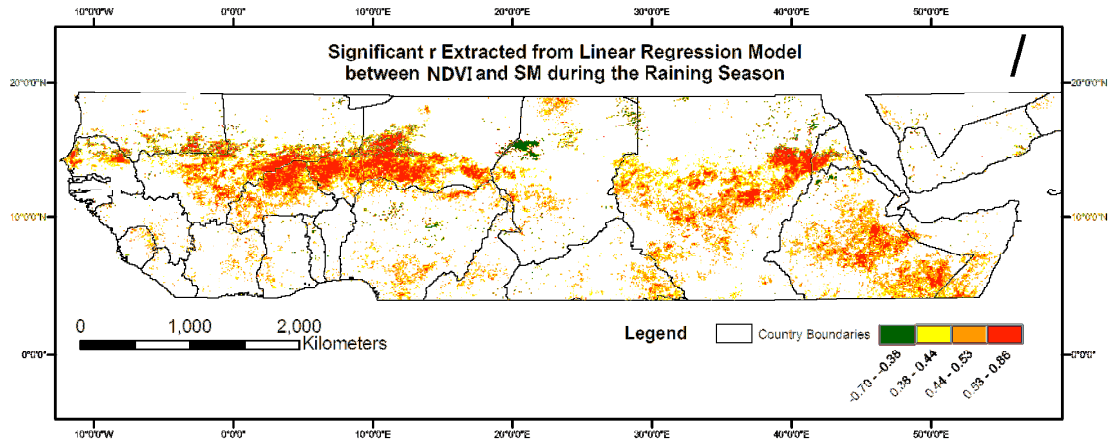

Figure 2. r image calculated from the linear regression analysis, and pixels are extracted at significant level (r>=0.381 and r<=-0.381), with α=0.05

Inspection of the images reveals that r values are clustered either in high positive values or low negative values across Sahel at continental level. This spatial pattern indicates that a linear relationship exists between NDVI and Soil Moisture at a statistically significant level of -0.381 or 0.381. Thus, the original data sets are claimed to satisfy the first assumption of linear regression, and can be kept as candidates for further check on other assumptions.

The second assumption is stated as,
The errors (i.e., the residuals) have mean zero, and constant variance; that is, $E[\varepsilon] = 0$ and $V[\varepsilon] = \sigma^2$. The errors about the regression line do not vary with x; that is, $V[\varepsilon|x] = \sigma^2 x = \sigma^2$.

After fitting the original data sets into the linear model, a time series of images which display residuals per pixel is produced. Then, a calculation of the average of the set of residuals is conducted, thus to test the assumptions of $E[\varepsilon] = 0$.

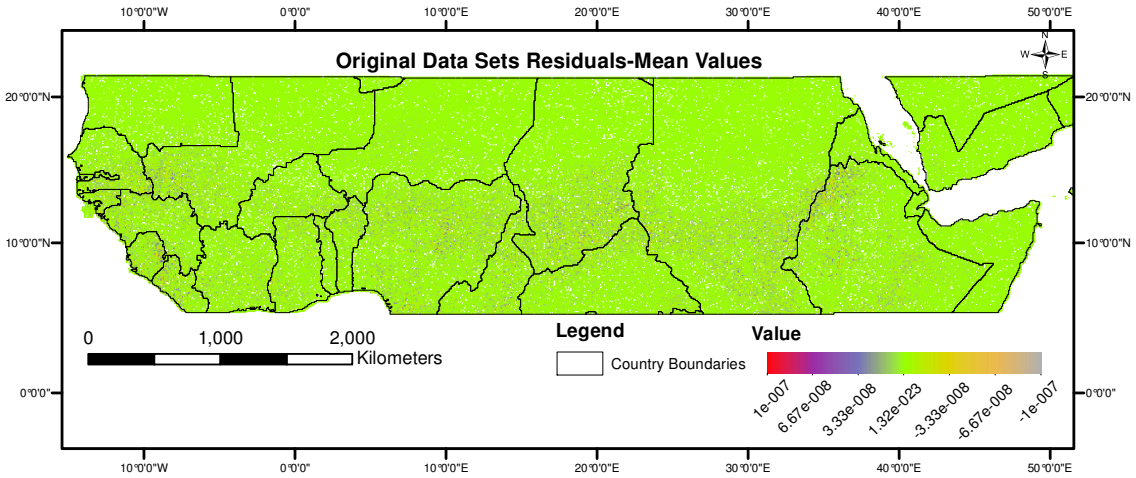

Figure 3. Average residual values per pixel over the 27-year period.

According to Figure (3), the original data sets have average residuals around zero for most of their pixels. Even with non-zero values, the deviations from zero are trivial. To conclude, the original data sets have satisfied the condition of having all their error terms with a-zero-mean.

To test for the constant variance criteria of the second assumption, studentized Breusch-Pagan test is applied in R. Notice that R has its own limitation in handling large amount of data, it is impossible for R to perform the test for all the pixels in the study area throughout the 27-year period. Therefore, 19 randomly sampled pixel points are generated covering most of the study area (Figure 4). At each sample point, studentized Breusch-Pagan tests are carried out in R and the results are shown in table (5).

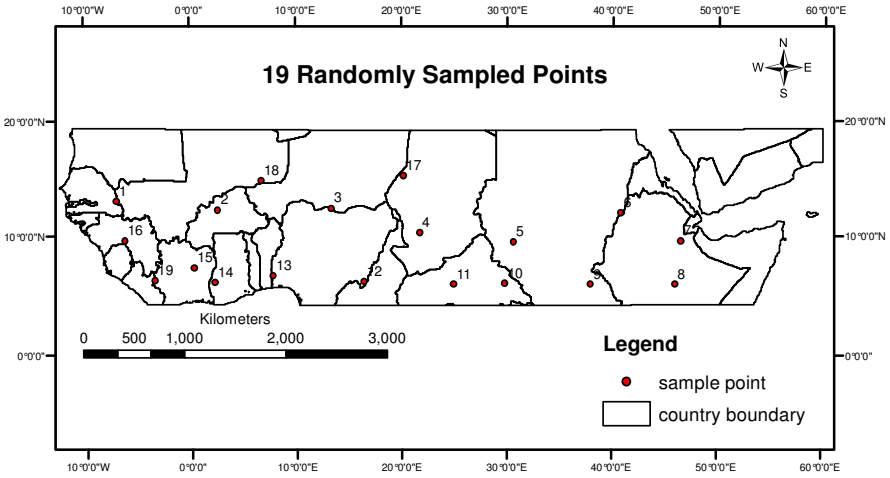

Figure 4. Sample points selected for the Breusch-Pagan tests.

Table 5. Studentized Breusch-Pagan test, "✓" pass; "✓" refers to the one with highest test result; "X" fail.

Sample Points / Studentized Breusch-Pagan Test	1	2	3	4	5	6	7	8	9	10	11	12	13	14	15	16	17	18	19
Original	√	×	√	√	√	√	√	√	×	√	√	√	√	√	√	√	√	√	√

The test results in table (5) show that samples selected from the original datasets have 2 fails and 17 passes in the overall result. In general, despite of the 2 fails, the majority of sample points have passed the test. Therefore, it is speculated that the majority of the whole data sets do not violate this assumption.

The third assumption requires that the residuals are independent implying that the value of one error is not affected by the value of another error.

In order to test the independence, of the residuals, Durbin-Waston statistics are used to conduct the test.

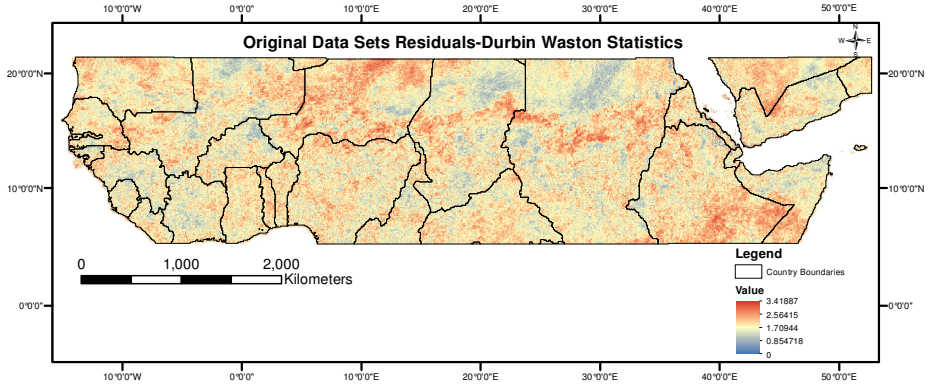

Figure 5. Durbin Waston statistics for the residuals of original data sets.

The Durbin Waston Statistics with value 2 indicates no serial autocorrelation; less than 2 indicates evidence of a positive serial correlation and statistic greater than 2 indicates evidence of a negative serial autocorrelation. The test results displayed in Figure (5) have revealed that most of the statistics are close to value 2. The average statistics for the entire study area is listed out in table (6).

Table 6. Average Durbin Waston statistics for the residuals of original data sets.

Data Sets	Population Size N	Mean Test Result	Standard Deviation
Original	182737	1.837	0.421

Nevertheless, with the mean test results 1.837 close to 2, but not exactly at 2, it may seem controversial to accept such a result. Therefore, a trend preserving and prewhitening process was implemented for the original data sets, which preserves the trend in the original series, but cleans up the correlations. Then, compare the Durbin Waston test results are compared between the prewhitened and the original residual time series in order to explore the validity of the original data sets.

Table 7. Durbin Waston test results for residuals calculated from the original data sets and residuals calculated after the prewhitening operations.

Data Sets	Population Size N	Mean Test Result	Standard Deviation
Original	182737	1.837	0.421
Original Prewhitened	182737	1.854	0.319

From table (7), the test results show that although the autocorrelation was removed from the residual time series, the mean test result of the prewhitened residual time series is similar to the original residual time series. Thus, the original data sets can be accepted with confidence.

To conclude, except the fourth assumption which is not testable with the small amount of time series data processed in this study, all the other three assumptions were checked under different statistical tests. The test results have proven that the original data sets satisfy all the assumptions listed out in the simple linear regression analysis, therefore it is reasonable to use these data sets in the following studies.

4.2 Memory Effects in Sahel

4.2.1 Finding Memory Effects

After regressing the residual time series with different soil moisture at tri-monthly periods with different time lags, it is showing that the average R^2 value is most comparably high at SM(9-7)_1 and SM(3-1)_2 (Figure 6). Notice that the average R^2 values were averaged out over the entire study period, including areas with 0 values and non-significant R^2 values, therefore, these values are rather small, however, one shall only look at its trends, and allocate the highest R^2 values in comparison with others.

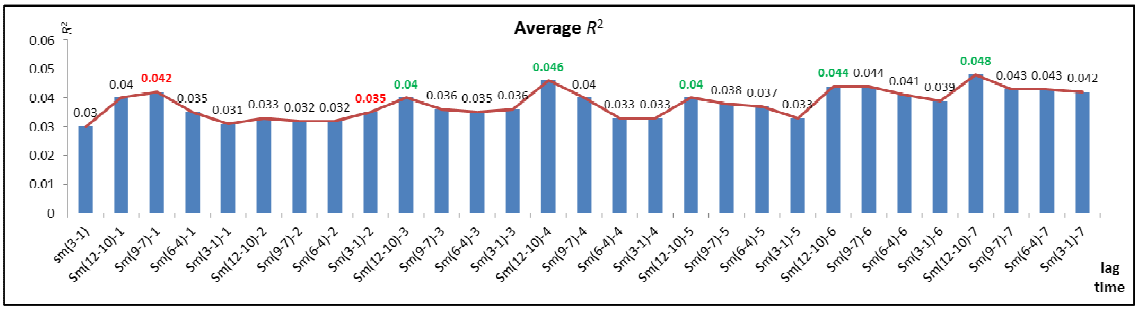

Figure 6. Average R^2 over the entire study area from linear regression models between NDVI residuals and soil moisture content with different time lags. Numbers in Red outlines the highest values within the two-year time lag; Numbers in Green outlines the highest values from three-year to seven-year time lags.

From Figure (6), it is hypothesized based on Richard et al (2008)'s method that two memory effects exist in the study area by selecting the highest average R^2 values. They are labelled in red. One memory effect is found at one-year time lag, from month July to September. The second memory effect is found at the two-year time lag, which appears at the tri-monthly period between January and March. From then on, peaks always appear at October to December in a cyclic fashion.

Besides comparing the average R^2 values among different time lags, areas which contain R^2 values equal and greater than the significant R^2 values (table 8) are counted and compared with the area of the whole study region. The results are presented in percentages at Figure (7).

Table 8. Minimum r and R^2 values at different sample size required for significance, using student's two tailed t test, with α=0.05.

Sample Size(number of years)	Time Lag	Minimum Absolute Value of r Required for Significance(using student's two tailed t test, with α=0.05)	Minimum R2 needed to attain significance (square of r significance)
n= 27	Concurrent Year	0.381	0.145
n= 26	One Year Before	0.388	0.151
n= 25	Two Years Before	0.396	0.157
n= 24	Three Years Before	0.404	0.163
n= 23	Four Years Before	0.413	0.171
n= 22	Five Years Before	0.423	0.179
n= 21	Six Years Before	0.433	0.187
n= 20	Seven Years Before	0.444	0.197

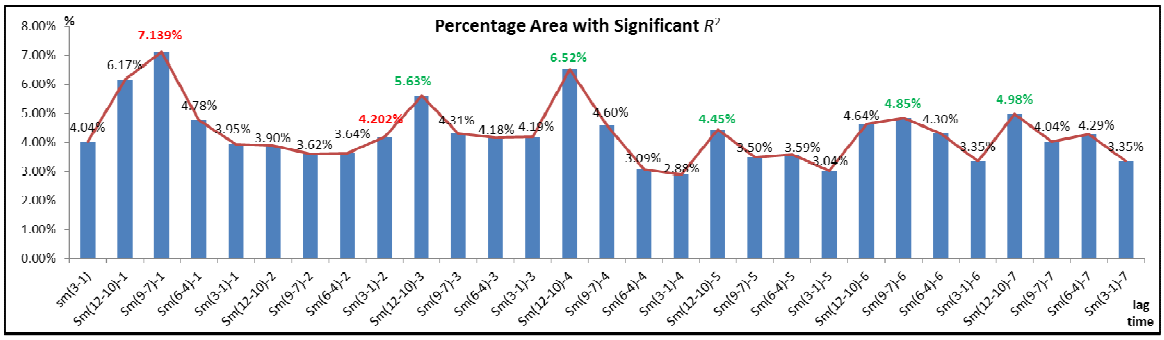

Figure 7. Area in percentage of significant R^2 over each linear regression between NDVI residuals and soil moisture content with different time lags.

Figure (7) resembles a same fashion in trend as in Figure (6), with two anomalies (labelled in red) comparably high with respect to the other values in different time lags. Remarkably, one of these values (7.139%) is found as the highest one among all the values in the table, which can be served as a certification for claiming the memory effect in this time lag.

To conclude, the two peaks found in R^2 values at different time lag and tri-monthly period indicate the existence of two memory effects in the study area. However, the second memory effect is rather weak compare to the first one, thus, only look into the first memory effect at the following studies.

In the following studies, this memory effect is referred to as mem7-9, which represents a 7-to-9 month lag effect of soil moisture acting upon NDVI.

4.2.2 mem7-9 stratification

The overall residual time series were further divided into positive and negative residual time series, and the two categories were regressed with SM(9-7)_1, respectively. The spatial locations with significant R^2 values are displayed in Figure 8.

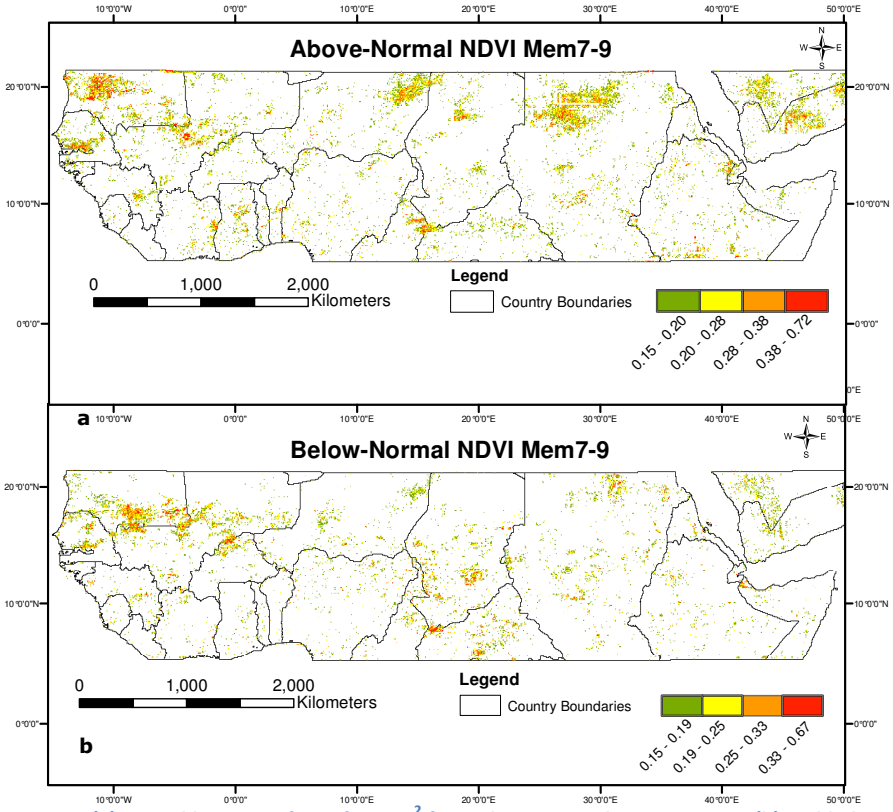

Figure 8. (a) Spatial location of significant R^2 from above-normal NDVI mem7-9 (b) and below-normal NDVI mem7-9; level of significance: R^2=0.151, with α=0.05.

According to Figure (8), mem7-9 explains the above-normal NDVI (above-normal mem7-9) and is mostly located on the west and northern-west corner, upper and lower middle parts of the Sahel. The associated countries are Mauritania, Senegal and Mali, Guinea, and Ghana (west and northern-west corner), Niger, Chad and Sudan (upper middle), overlapping with Chad, Central African Republic and Cameroon (lower middle). On the other hand, mem7-9 which explains for the below-normal NDVI (below-normal mem7-9) has most of its effect on the north-west (belt-shaped) corner, middle to lower-middle, and east part of Sahel. The associated countries are Mauritania, Senegal, and Mali (northern-west belt), Niger, Chad and Central African Republic (middle to lower middle), Sudan (east). Notice that the Arabia Peninsula is excluded from the studying area, and therefore can be ignored. The area of significant R^2 for both memory effects are listed in table (9).

Table 9. Percentage area of significant R^2 of both above-normal mem7-9 and below-normal mem7-9.

Type of Memory Effect	Effective Area
Above-Normal Mem7-9	7.401%
Below-Normal Mem7-9	5.148%

14 sample points which are selected based on Figure (8a) is presented in Figure (9).

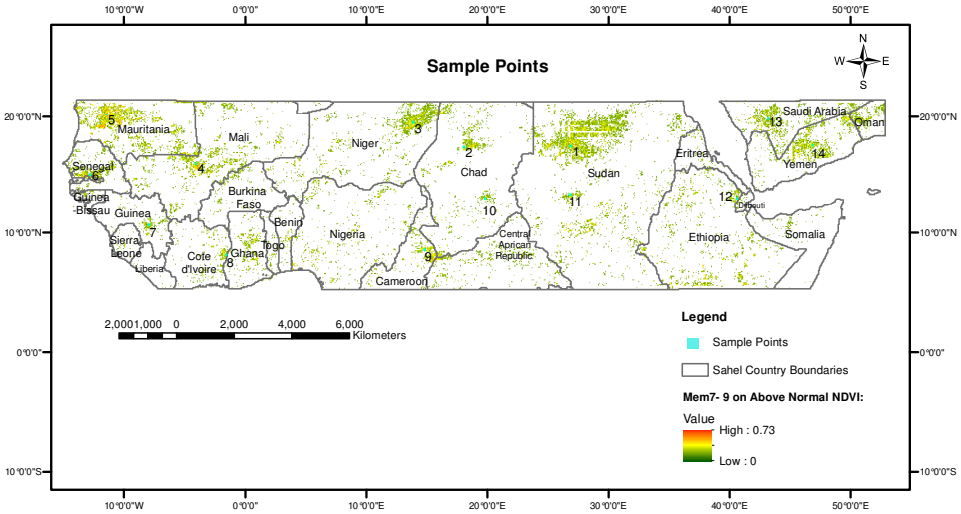

Figure 2. Sample points selected from above-normal NDVI mem7-9 image (Figure 8a).

15 sample points which are selected based on Figure (8b) is presented in Figure (10).

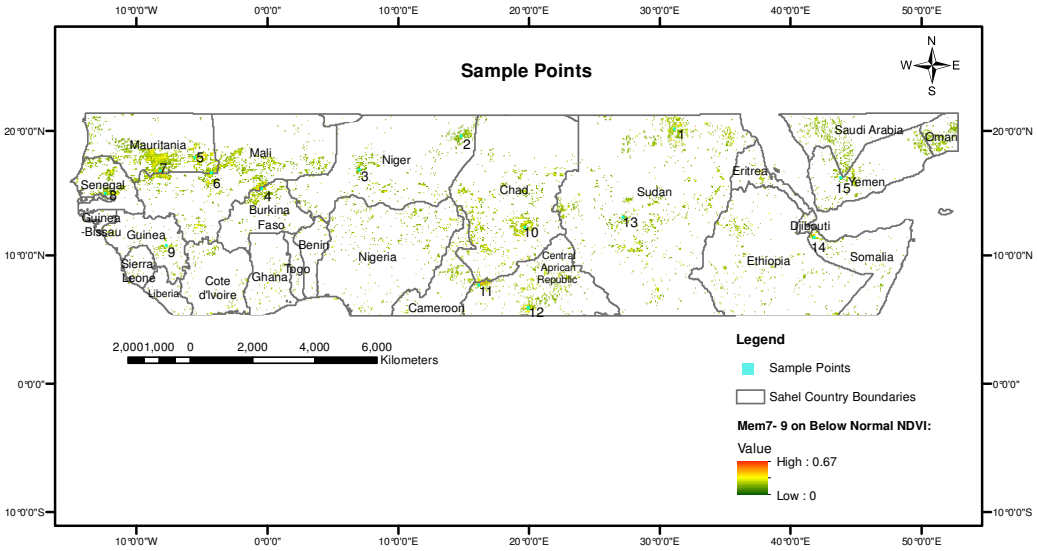

Figure 10. Sample points selected from below-normal NDVI mem7-9 image (Figure 8b).

After the selection of sample points, R^2 values calculated from linear regressions between the residual time series and soil moisture contents with time lags for each sample point are graphed out in Figure (11) and (12).

Observed from Figure (11), all the 14 samples show similarities in their graphs from SM (3-1) to SM (3-1_2), that is soil moisture content from January till March at concurrent years and soil moisture content from January till March with two-year time lags. After the two-year time lags (in red line of Figure 11), the R^2 values tend to fluctuate and differ among the 14 samples. Within the two-year time lags, the general trend shows that R^2 gradually reaches its highest values at SM (9-7_1), before starting to drop dramatically after the peak. Some exceptions are also observed within the two-year time lags. One exception is found in sample point 8a, where two peaks with slightly different values are shown (0.33, 0.32), at SM (9-7_1) and SM (6-4_2) respectively. Another exception is involved with sample 3a and 11a, in which the peaks appear at SM (12-10_1) instead of SM (9-7_1).

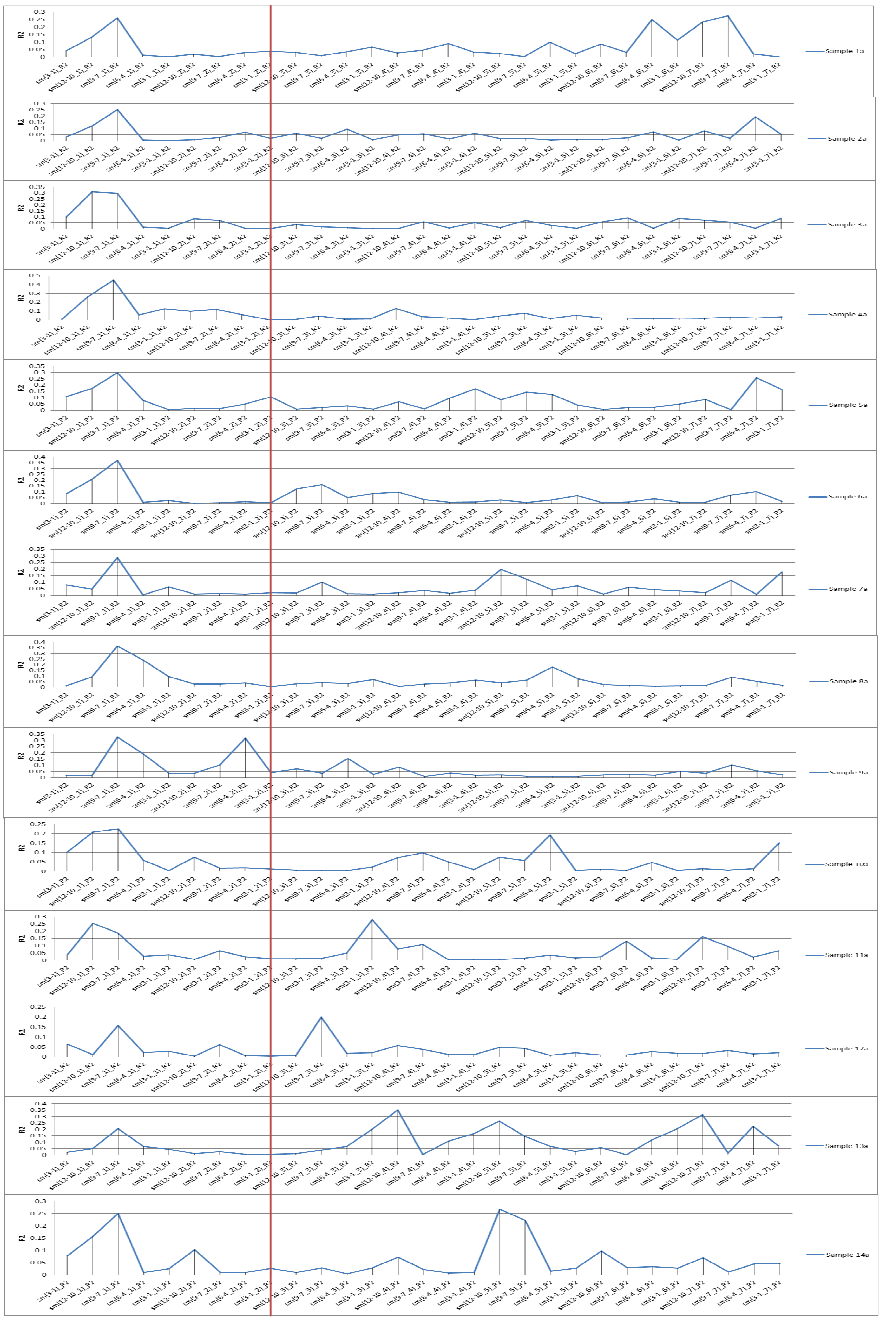

Figure 11. R^2 from linear regression models between NDVI residuals and soil moistures with time lags on samples selected from figure (9a). The Red Line represents the two-year time lag.

Figure (12) presents R^2 of sample points selected from clusters in mem7-9 on below-normal NDVI residuals, likewise Figure (11), the graphs for all the 15 sample points have a similar profile between SM (3-1) and SM (3-1_2), which is a two-year time lag. The rest of the profiles are considered as fluctuations, without obvious trends. Within the two-year time lag, exceptions are found in sample point 3b, 10b and 13b, of which R^2 peak at SM (12-10_1) instead of SM (9-7_1). Moreover, for most of the samples, the R^2 values reach to the peaks at SM(9-7_1), then gradually trail off, however, for sample point 10b, it has two cycles within the two-year time lag, and the peaks of the two cycles are at SM (12-10_1) and SM (9-7_2), respectively.

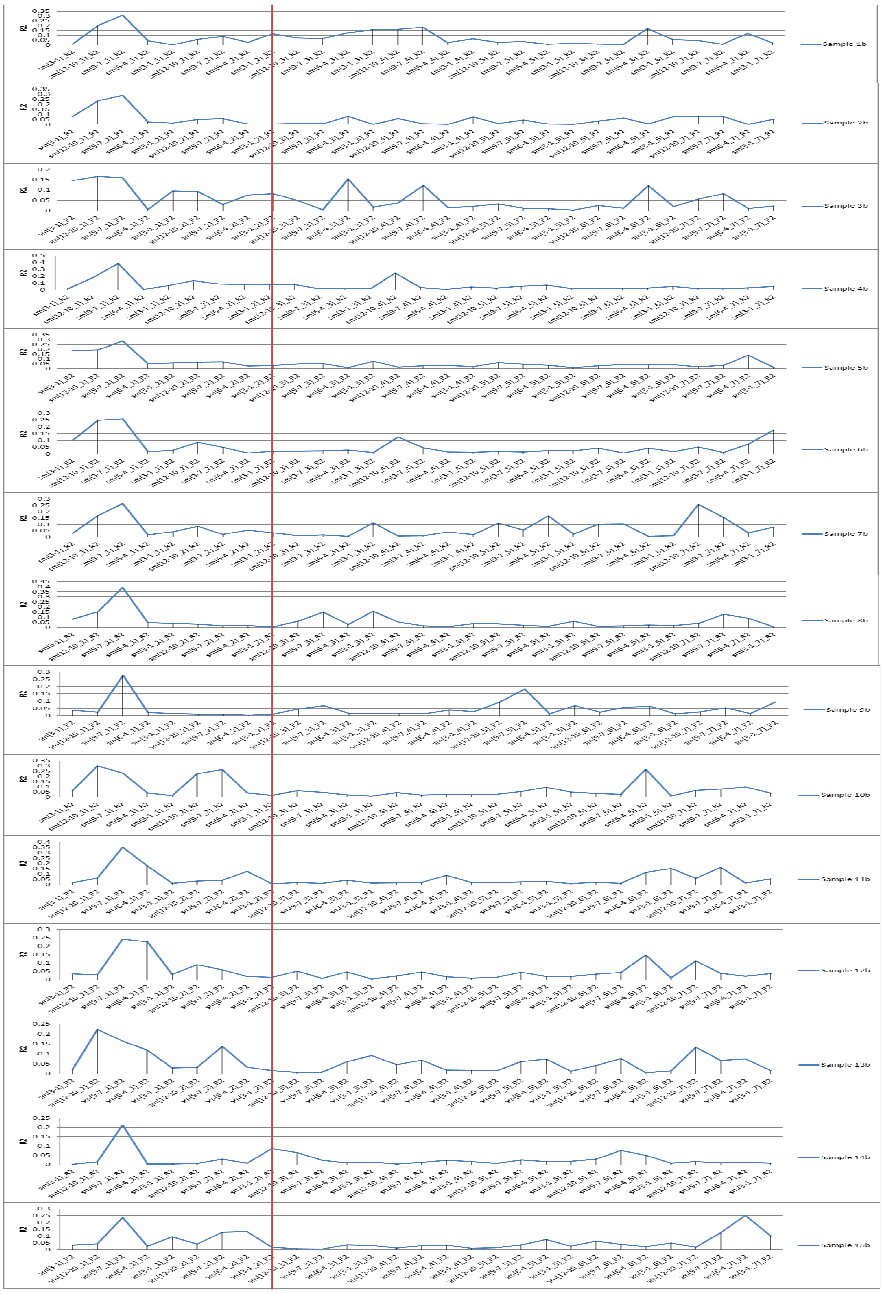

Figure 12. R^2 from linear regression models between NDVI residuals and soil moistures with time lags on samples selected from figure (9b). The Red Line represents the two-year time lag.

Figure (13) and (14) are plotted to show the highest R^2 values for each sample point within the two-year time lags. Notice that in both sample sets, sample points 4a and 8b have the highest R^2 values compare to other sample points. The lowest sample points are 12a and 3b. The average R^2 of each sample are 0.29 and 0.28, respectively.

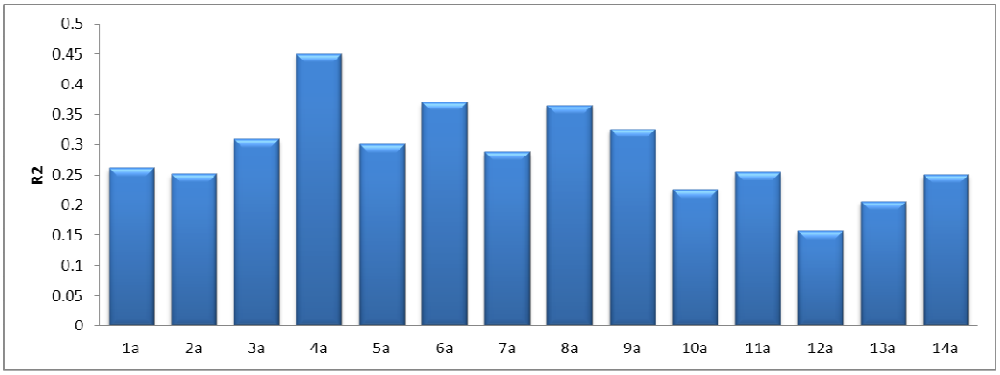

Figure 13. Maximum R^2 of samples selected from figure (9a) over the two-year time lags.

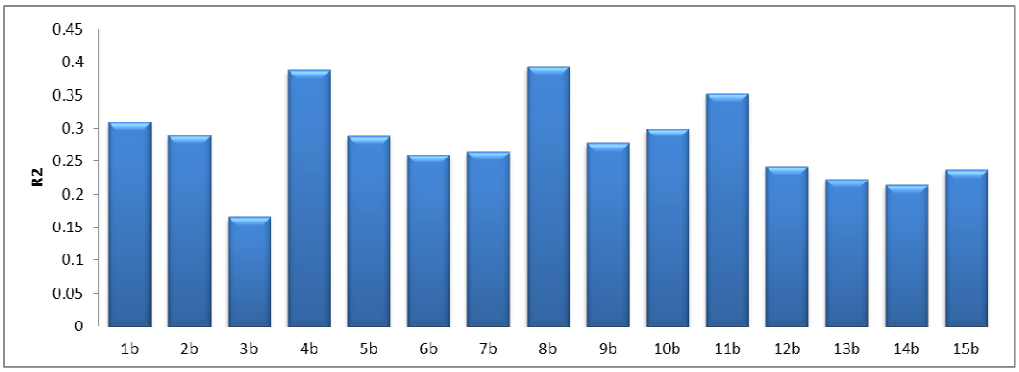

Figure 14. Maximum R^2 of samples selected from figure (9b) over the two-year time lags.

The land cover types and soil types associated with each sample points are presented in table (10) and (11).

Table 10. Land cover and soil type for each sample point selected from Figure (8a).

Samples	Land Cover Type	Soil Type	Soil Texture
sample 1a	Sandy desert and dunes	Rock	
	Stony desert	Aridisols	stony
sample 2a	Sandy desert and dunes	Shifting Sand	
sample 3a	Sandy desert and dunes	Shifting Sand	
sample 4a	Closed grassland	Vertisols	clayey
	Open grassland with sparse shrubs	Alfisols	clayey
	Open grassland		
sample 5a	Sandy desert and dunes	Shifting Sand	
	Stony desert	Entisols	fine sandy and clayey
sample 6a	Croplands (>50%)	Alfisols	clayey
	Croplands with open woody vegetation	Entisols	fine sandy and clayey
sample 7a	Mosaic Forest / Croplands	Ultisols	clayey
	Deciduous woodland		
sample 8a	Mosaic Forest / Croplands	Ultisols	clayey
	Deciduous shrubland with sparse trees		
sample 9a	Deciduous woodland	Entisols	fine sandy and clayey
	Deciduous shrubland with sparse trees		
sample 10a	Croplands with open woody vegetation	Alfisols	clayey
sample 11a	Open grassland	Shifting Sand	
	Sparse grassland		
	Bare rock		
sample 12a	Bare rock	Entisols	fine sandy and clayey
sample 13a	N/A	Shifting Sand	
sample 14a	N/A	Aridisols	stony
		Aridisols	stony

Table 11. Land cover and soil type for each sample point selected from Figure (8b).

Samples	Land Cover Type	Soil Type	Soil Texture
sample 1a	Sandy desert and dunes	Rock	
	Stony desert	Aridisols	stony
sample 2a	Sandy desert and dunes	Shifting Sand	
sample 3a	Sandy desert and dunes	Shifting Sand	
sample 4a	Closed grassland	Vertisols	clayey
	Open grassland with sparse shrubs	Alfisols	clayey
	Open grassland		
sample 5a	Sandy desert and dunes	Shifting Sand	
	Stony desert	Entisols	fine sandy and clayey
sample 6a	Croplands (>50%)	Alfisols	clayey
	Croplands with open woody vegetation	Entisols	fine sandy and clayey
sample 7a	Mosaic Forest / Croplands	Ultisols	clayey
	Deciduous woodland		
sample 8a	Mosaic Forest / Croplands	Ultisols	clayey
	Deciduous shrubland with sparse trees		
sample 9a	Deciduous woodland	Entisols	fine sandy and clayey
	Deciduous shrubland with sparse trees		
sample 10a	Croplands with open woody vegetation	Alfisols	clayey
sample 11a	Open grassland	Shifting Sand	
	Sparse grassland		
	Bare rock		
sample 12a	Bare rock	Entisols	fine sandy and clayey
sample 13a	N/A	Shifting Sand	
sample 14a	N/A	Aridisols	stony
		Aridisols	stony

Observed in table (10), the dominant land cover types among the samples are croplands, deciduous woodland and shrubland, and sandy deserts and dunes while the dominant soil types are Entisols and Shifting Sand. Observed in table (11), the dominant land cover types among the samples are grassland and croplands; the dominant soil types are Entisols and Alfisols.

Furthermore, positive and negative r is differentiated for the above-normal mem7-9 and below-normal mem7-9, respectively. The spatial locations are shown in Figure (15) and (16).

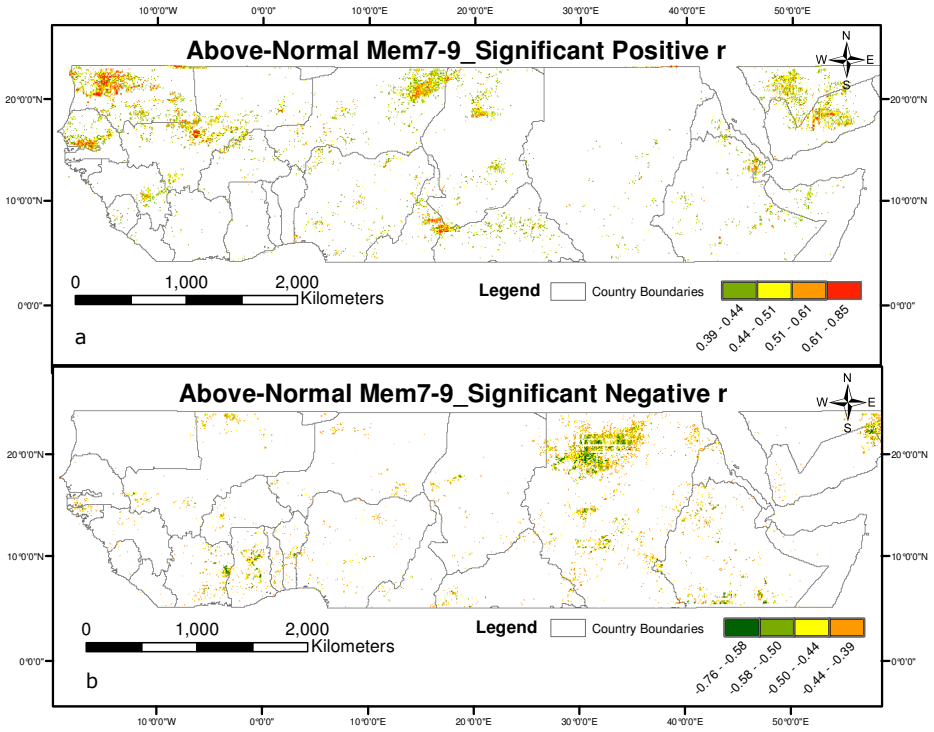

Figure 15. (a) Spatial location of significant positive r from above-normal mem7-9 (Scenario 1); (b) spatial location of significant negative r from above-normal mem7-9 (Scenario 2); level of significance: r=0.388, with α=0.05.

From Figure (15a), the significant positive r values from the above-normal mem7-9 are mostly found in the north-west corner, and upper and lower middle part of the Sahel whereas the significant negative r values Figure (15b) are found mostly in the countries alongside the Gulf of Guinea, in the middle and northern part of Sudan. Notice that the Arabia Peninsula are excluded in the study area, therefore can be ignored.

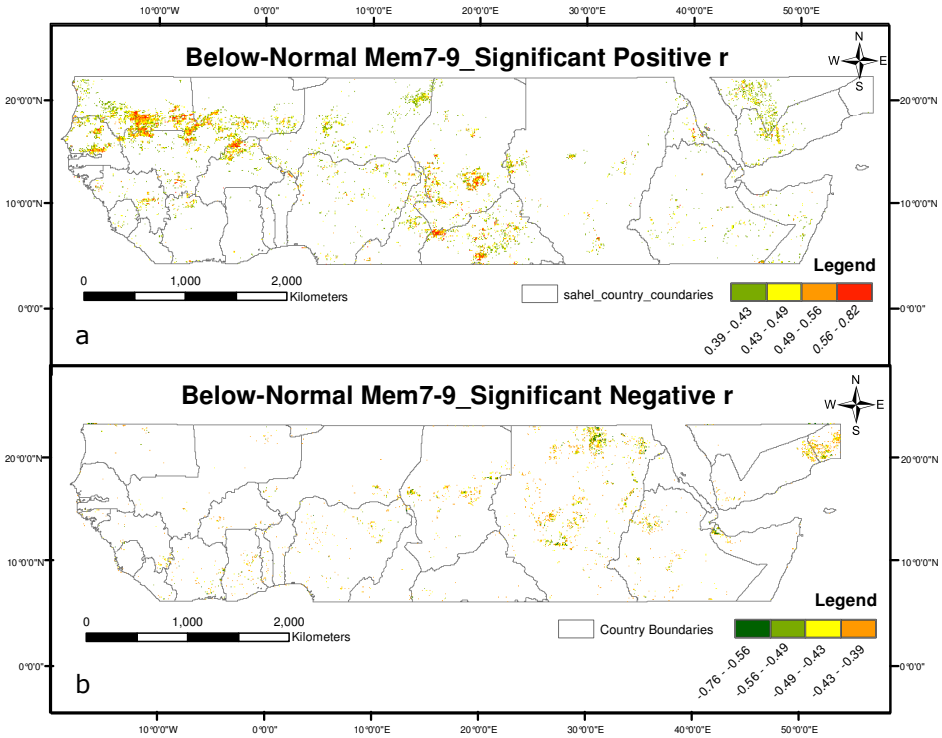

Figure 16. (a) Spatial location of significant positive r from below-normal mem7-9 (Scenario 3); (b) spatial location of significant negative r from below-normal mem7-9 (Scenario 4); level of significance: r=0.388, with α=0.05.

According to the spatial pattern displayed in Figure (16a), for below-normal NDVI mem7-9, significant positive r values are mostly horizontally distributed in the northern-west part, and clustered in the lower middle and northern-east part of Sahel. For the significant negative r values Figure (16b), they can be found in relatively large concentration at the middle part of Chad, upper and middle part of Sudan and northern-east part next to the Gulf of Omen.

4.3 Land Cover and Soil Type Association with the Four Scenarios

Only the top five land cover types as well as their associated soil types for each scenario are listed in table 12, 13, 14, and 15. In total, there are 7 land cover types and 10 soil types found to be most related to the mem7-9 effects.

For scenario 1, the dominant vegetation with descending sequence are crops, woody plants and grasses, and the dominate soil types for most of these vegetation types are Entisols and Alfisols.

Table 12. Land cover types and soil types found in Scenario 1. Both were ranked from High to low according to their relative percentages.

Scenario 1	**Above-normal Mem7-9**				
positive significant r	Implication: as SM **increases**, above-normal NDVI also **increases**; as SM **decreases**, above-normal NDVI also **decreases**				
Ranking	Land Cover Name	Land Cover type-Area in Percentage	Soil Type Name	Soil Type Texture	Soil Type-Area in Percentage
1	Croplands (>50%)	11.175%	Entisols	fine sandy and clayey	37.578%
			Alfisols	clayey	33.901%
			Inceptisols	clayey	13.453%
			Vertisols	clayey	6.547%
			Ultisols	clayey	6.278%
			Aridisols	stony	1.704%
			Shifting Sand		0.538%
2	Deciduous woodland	9.238%	Entisols	fine sandy and clayey	32.978%
			Ultisols	clayey	30.309%
			Oxisols	fine sandy	23.906%
			Alfisols	clayey	10.352%
			Inceptisols	clayey	2.241%
			Vertisols	clayey	0.213%
3	Open grassland with sparse shrubs	8.040%	Entisols	fine sandy and clayey	51.314%
			Alfisols	clayey	22.904%
			Shifting Sand		7.635%
			Inceptisols	clayey	6.884%
			Aridisols	stony	5.757%
			Vertisols	clayey	5.382%
			Ultisols	clayey	0.125%
4	Croplands with open woody vegetation	7.594%	Alfisols	clayey	47.051%
			Entisols	fine sandy and clayey	36.410%
			Vertisols	clayey	11.538%
			Inceptisols	clayey	2.564%
			Ultisols	clayey	2.051%
			Aridisols	stony	0.385%
5	Sparse grassland	6.320%	Entisols	fine sandy and clayey	62.303%
			Aridisols	stony	28.233%
			Shifting Sand		5.678%
			Vertisols	clayey	1.420%
			Alfisols	clayey	1.262%
			Inceptisols	clayey	1.104%

For scenario 2, the dominant vegetation types with descending sequence are woody plants, trees and crops, and the dominate soil type for most of these vegetation types is Alfisols.

Table 13. Land cover types and soil types found in Scenario 2. Both were ranked from High to low according to their relative percentages.

Scenario 2	**Above-normal Mem7-9**				
negative significant r	Implication: as SM **increases**, above-normal NDVI **decreases**; as SM **decreases**, above-normal NDVI **increases**				
Ranking	Land Cover Name	Land Cover type-Area in Percentage	Soil Type Name	Soil Type Texture	Soil Type-Area in Percentage
1	Deciduous woodland	9.147%	Alfisols	clayey	55.292%
			Oxisols	fine sandy	17.378%
			Ultisols	clayey	11.848%
			Entisols	fine sandy and clayey	11.374%
			Inceptisols	clayey	3.002%
			Vertisols	clayey	0.790%
			Andisols	loam	0.316%
2	Deciduous shrubland with sparse trees	8.462%	Alfisols	clayey	34.471%
			Entisols	fine sandy and clayey	26.109%
			Vertisols	clayey	18.771%
			Inceptisols	clayey	10.751%
			Ultisols	clayey	8.020%
			Andisols	loam	1.024%
			Oxisols	fine sandy	0.853%
3	Croplands (>50%)	6.455%	Entisols	fine sandy and clayey	32.880%
			Inceptisols	clayey	25.850%
			Vertisols	clayey	14.966%
			Alfisols	clayey	12.472%
			Ultisols	clayey	9.297%
			Andisols	loam	3.401%
			Aridisols	stony	0.907%
			Oxisols	fine sandy	0.227%
4	Croplands with open woody vegetation	6.104%	Vertisols	clayey	34.048%
			Alfisols	clayey	26.429%
			Entisols	fine sandy and clayey	24.762%
			Inceptisols	clayey	9.762%
			Ultisols	clayey	3.571%
			Aridisols	stony	0.952%
			Oxisols	fine sandy	0.476%
5	Mosaic Forest / Croplands	4.682%	Ultisols	clayey	64.615%
			Alfisols	clayey	19.385%
			Inceptisols	clayey	8.923%
			Oxisols	fine sandy	4.923%
			Entisols	fine sandy and clayey	1.846%
			Andisols	loam	0.308%

For scenario 3, the dominant vegetation types with descending sequence are crops, grasses and woody plants, and the dominate soil types for most of these vegetation types are Entisols and Alfisols.

Table 14. Land cover types and soil types found in Scenario 3. Both were ranked from High to low according to their relative percentages.

Scenario 3	**Below-normal Mem7-9**				
positive significant r	Implication: as SM **increases**, below-normal NDVI also **increases**; as SM **decreases**, below-normal NDVI also **decreases**				
Ranking	Land Cover Name	Land Cover type-Area in Percentage	Soil Type Name	Soil Type Texture	Soil Type-Area in Percentage
1	Croplands (>50%)	17.971%	Entisols	fine sandy and clayey	51.986%
			Alfisols	clayey	28.690%
			Vertisols	clayey	7.232%
			Inceptisols	clayey	6.935%
			Ultisols	clayey	2.608%
			Shifting Sand		1.838%
			Aridisols	stony	0.652%
			Oxisols	fine sandy	0.059%
2	Sparse grassland	12.981%	Entisols	fine sandy and clayey	72.539%
			Aridisols	stony	16.708%
			Shifting Sand		8.271%
			Inceptisols	clayey	0.910%
			Alfisols	clayey	0.827%
			Vertisols	clayey	0.579%
			Ultisols	clayey	0.165%
3	Croplands with open woody vegetation	11.849%	Alfisols	clayey	50.721%
			Entisols	fine sandy and clayey	32.883%
			Vertisols	clayey	10.541%
			Ultisols	clayey	3.153%
			Inceptisols	clayey	2.162%
			Aridisols	stony	0.541%
4	Open grassland with sparse shrubs	10.540%	Entisols	fine sandy and clayey	59.857%
			Alfisols	clayey	19.305%
			Shifting Sand		10.215%
			Vertisols	clayey	5.005%
			Aridisols	stony	4.290%
			Inceptisols	clayey	1.021%
			Ultisols	clayey	0.306%
5	Deciduous woodland	9.231%	Oxisols	fine sandy	37.631%
			Entisols	fine sandy and clayey	28.688%
			Ultisols	clayey	21.719%
			Alfisols	clayey	10.221%
			Inceptisols	clayey	1.742%

For scenario 4, the dominant vegetation types with descending sequence are crops, woody plants, and grasses, and the dominate soil types for most of these vegetation type are Entisols, Vertisols and Alfisols.

Table 15. Land cover types and soil types found in Scenario 4. Both were ranked from High to low according to their relative percentages.

Scenario 4	**Below-normal Mem7-9**				
negative significant r	Implication: as SM **increases**, below-normal NDVI **decreases**; as SM **decreases**, below-normal NDVI **increases**				
Ranking	Land Cover Name	Land Cover type-Area in Percentage	Soil Type Name	Soil Type Texture	Soil Type-Area in Percentage
1	Croplands (>50%)	11.132%	Entisols	fine sandy and clayey	29.771%
			Vertisols	clayey	23.664%
			Alfisols	clayey	16.285%
			Inceptisols	clayey	14.249%
			Ultisols	clayey	13.995%
			Aridisols	stony	1.018%
			Shifting Sand		1.018%
2	Croplands with open woody vegetation	8.621%	Vertisols	clayey	40.893%
			Alfisols	clayey	25.430%
			Entisols	fine sandy and clayey	24.055%
			Inceptisols	clayey	7.560%
			Ultisols	clayey	1.031%
			Aridisols	stony	0.687%
			Mollisols	clayey	0.344%
3	Sparse grassland	7.309%	Shifting Sand		63.241%
			Aridisols	stony	17.787%
			Entisols	fine sandy and clayey	13.834%
			Vertisols	clayey	5.138%
4	Deciduous shrubland with sparse trees	6.597%	Alfisols	clayey	44.954%
			Vertisols	clayey	19.725%
			Entisols	fine sandy and clayey	15.138%
			Inceptisols	clayey	11.468%
			Ultisols	clayey	7.798%
			Aridisols	stony	0.459%
			Oxisols	fine sandy	0.459%
5	Open grassland with sparse shrubs	6.484%	Shifting Sand		51.351%
			Entisols	fine sandy and clayey	19.369%
			Vertisols	clayey	9.910%
			Alfisols	clayey	9.910%
			Aridisols	stony	5.405%
			Inceptisols	clayey	2.703%
			Ultisols	clayey	1.351%

Chapter 5: Discussion

5.1 Time lags of the Memory effects

Results of this study have shown a 7-to-9 month time lag which is found from high R^2 values between NDVI residuals and soil moisture content. Compared to the work done by Richard et al in 2008, results show similarities between one another. Their work has focused in the semi-arid region in South Africa during the austral early summer (September-December). Results have shown two memory effects in their studies, one is called mem1 and is associated with lag effects between NDVI difference from September to December ($NDVI_{D-S}$) and September to November NDVI values of the preceding year ($NDVI_{son-1}$); the other one is called mem2 and is associated with lag effects between $NDVI_{D-S}$ and precipitation accumulated from the January to April of the preceding summer PP_{JFMA} (Richard et al., 2008). To compare, only look at mem2 due to the comparability between rainfall and soil moisture data. In mem2, rainfall in the last period of the rainy season controls (beyond the intervening dry season) the inter-annual variations of NDVI (December to September) at the beginning of the next rainy season (Richard et al, 2012). Moreover, it had a negative correlation between rainfall and the greenness difference which implies that above normal rainfall from January to April is statistically associated with negative anomalies of the greenness development 7-10 months later (Richard et al. 2008). By comparison, the time lag periods between the two studies seem to confirm each other. However, both positive and negative relationships are found between NDVI and soil moisture data in this study, due to the large size of study area as well as spatial heterogeneity.

In the studies of Phillippon et al. (2005), (although using a different approach) results are similar compared to this study. Their study area was located in West Africa including parts of Sahel and Guinea, thus comprising both semi-arid and temperate climates. Instead of using cross correlations, Phillippon et al. (2005) use serial correlation to assess similarity at a given time lag for each of the variables (Phillippon et al, 2005). Thus, results have shown that NDVI or soil-vegetation water content (sigma_0) anomalies observed in the raining season (September-October) have high correlations with observations 7 to 9 months later (April-June). Nevertheless, analysis from this paper also indicates a high correlation between NDVI and sigma_0 within the study area of Sahel (R^2=0.8). This implies a high similarity in the evolution of time series between the two variables. Although not concluded by the author, it can be argued that the two time series are interchangeable. Additionally, Ahmed (2012) compares different lag effects between soil moisture and NDVI (same

data sets as used in this study), in Sahel at the sub-continental level. Results have indicated that lag0, has the highest correlations over the region (r varies between 0.1-0.6) compared to the others. Therefore it is valid to replace NDVI with sigma_0 or soil moisture data and to claim that sigma_0 anomalies or soil moisture data are significantly linked to NDVI anomalies in the up-coming spring (7-to-9 month later). The results from Philippon et al. (2005) and Ahmed (2012) therefore could be used to testify to the validity of the time lag periods found in this paper.

5.2 Memory effects and its Spatial Patterns

Results from the memory effect analysis have shown locations where memory effects are strongest across the study area. To further analyse the above-normal NDVI mem7-9 and below-normal NDVI mem7-9, they were further divided by extracting both the positive r and negative r values from each image, thus creating the following four scenarios. The implication of each scenario is presented in Table 16.

Table 16. Implications of the four scenarios.

Memory Effects	Differentiation of r	Implications	Names
Above-normal NDVI Mem7-9	Significant Positive r	as SM **increases**, above-normal NDVI (positive residual) also **increases**; as SM **decreases**, above normal NDVI (positive residual) also **decreases**	Scenario 1
	Significant Negative r	as SM **increases**, above-normal NDVI (positive residual) **decreases**; as SM **decreases,** above normal NDVI (positive residual) **increases**	Scenario 2
Below-normal NDVI Mem7-9	Significant Positive r	as SM **increases**, below-normal NDVI (negative residual) also **increases**; as SM **decreases**, below normal NDVI (negative residual) also **decreases**	Scenario 3
	Significant Negative r	as SM **increases**, below-normal NDVI (negative residual) **decreases**; as SM **decreases,** below-normal NDVI (negativeresidual) **increases**	Scenario 4

The spatial pattern of above-normal residuals which are sensitive to soil moisture contents are mainly clustered in the northern Sahel between 15°N and 20°N (Figure 8a). This anomaly pattern can be accounted for by an earlier northward excursion of the ITCZ in the wet years, thus stimulating a longer rainy season at latitudes north of 10°N and leaving the southern region dry (Griffiths, 1972; Motha et al., 1980). However, the land cover types found in these areas are mainly sandy deserts and dunes, and stony desert. Therefore, the high R^2 in these areas might be due to data clustering. When data are similar in value or clustered, they can impose potential errors in regression analysis (Galbraith, 2010). Moreover, the spatial pattern observed in the below-normal NDVI residuals is partially concentrated in the centre of the southern Sahel; below latitude level 12°N (Figure

8b). This could be partially explained by NDVI anomalies observed in the dry years over the region. A noteworthy similarity of spatial distribution between the above-normal NDVI and below-normal NDVI residuals is apparent in the north-west corner as well as in the western part of the Sahel. Similar phenomenon can also be observed from the NDVI anomaly images summarized for corresponding dry and wet years in the paper by Anyamba and Tucker in 2005. In the very wet years, positive NDVI anomalies are mainly found in the upper Sahel between latitude 14°N and 18°N, which extends from the west to the east. Similarly, in dominant dry years, negative anomalies can also be found from the west till the east at the same latitude. Therefore, the west side of this area is vulnerable to rainfall changes, which results in the above-mentioned NDVI anomalies. In fact, the western parts of Sahel including countries of Senegal, Mauritania and Mali have shown variability of NDVI anomalies, according to Anyamba and Tucker (2005), might be caused by the maritime influence from the adjacent oceans.

Despite understanding the driving forces behind the spatial distribution of NDVI anomalies, it is nevertheless interesting to look at these spatial patterns individually, especially in areas with clusters. Thus, two sets of sample points are selected from the clusters in Figure 8a and 8b. Results of extracting the R^2 values for different trimestral soil moisture content with time lags for each sample are presented in Figures 11 and 12. According to Figure 11, two samples show an earlier memory effect than the rest of the samples for the above-normal NDVI anomalies. Specifically, sample points 3a and 11a are observed to have a high correlation between soil moisture content from October to December of one year ago and the positive NDVI residuals. This divergence in memory effect cannot be explained explicitly by the land cover types and soil types, as similar land cover types and soil types can be found in other samples but without the shifting of the memory effects. Results presented in Figure 12, which have three sample points showing the early shifting of memory effects, and again cannot be explained explicitly by either their land cover types or soil types. Nevertheless, two samples with the early shifts of memory effects are both found in Sudan, and they are sample 11a in Figure 9 and sample 13b in Figure 10. According to Heumann et al. (2007), phenology changes have mostly occurred in Soudan and Guinean regions between 1982 and 2005. In detail, phenological features such as seasonal NDVI amplitude (AMP) and length of the growing season (LGS) tend to increase with an increasing seasonally integrated NDVI (SiNDVI). Thus, the early shift memory effects might stimulate the positive NDVI anomalies which in return were captured in vegetation phenology changes , Again, an

early shift in memory effects associated with high latitude sample points, i.e. sample point 3a, cannot be explained and might be due to overfitting the regression models. Furthermore, two samples (sample 9a and 10b) from both sample sets have indicated a phenomenon of two cycles with maximum R^2 values showing in each cycle. When looking at the land cover and soil type for both of the samples, they are associated with woodland and shrubland, and with soil types Entisols and Ultisols. The reason why the memory effects are conspicuous over two periods might be explained by the physiological functionality of deep-rooted plants. As woody and herbaceous plants use water from different soil depths (Schenk and Jackson 2002, Moustakas et al, 2010), it enables them to transport water from deep soil layers stored in different times of years.

5.3 Memory effects related with Land Cover and Soil type

For the four scenarios, the memory effects are associated with different land covers and soil types, respectively. For scenario 1, where NDVI residuals are positive, if r values are within the range of positive significant level, then the land covers mostly found in this scenario are first of all crops, then woody plants, and finally grasses. The associated soil types are mainly Entisols and Alfisols, which have fine sandy or clayey features in their textures. Therefore, when NDVI is found to have above-normal levels, an increase in soil moisture level will also stimulate further growth of vegetation in the growing season if the land is covered by clayey soils and shallow-rooted plants such as crops and grasses. In addition, a decrease in soil moisture level will also hinder the further development of vegetation greenness with the above-mentioned land cover and soil types. It is demonstrated in the paper by Richard et al in 2012 that the vegetation type which is dominated by grass is more sensitive to rainfall changes than shrubs. Thus, for the shallow-rooted plants besides grass, they should also be sensitive to rainfall changes. Consequently, if soil moisture either increases or decreases, shallow-rooted plants should also follow the same trend seven to nine months later. Notice that the soil types under this scenario are both capable of holding water for long periods of time, e.g. up to 3 months for Alfisols (”The Twelve Orders of Soil Taxonomy”, n. d.) Therefore, they provide the right conditions for the development of a strong memory effect. For scenario 2, the negative r values between positive NDVI residuals and SM (7-9_1) are found to be mostly related to woody plants, trees and crops. Noticeably, the absence of grass and replacement of trees have indicated a change in land cover type for this scenario compared to scenario 1. Such a change in land cover type is evidenced by the work of Richard et al. (2012), which indicates a less sensitivity of NDVI to rainfall for vegetation types

dominated by shrubs. As a result, even NDVI is observed to be at above normal levels, an increase in soil moisture will not stimulate vegetation to develop further if the land is covered by shrubs or trees. Conversely, if soil moisture content is observed to be less than usual, vegetation such as shrubs or trees can still extract water from deeper layers, especially under the influence of "reverse hydraulic lift" (Richard et al, 2012). Therefore, with low soil moisture content, vegetation under scenario 2 will continue to grow, which may result in higher positive NDVI residuals.

In scenario 3 which contains below-normal NDVI values, mem7-9 was found mainly in vegetation types, including crops, grasses, and woody plants, in descending order. Similarly, scenario 4 is also composed of land cover types of crops, grasses and woody plants. However, soil types between the scenario 3 and 4are slightly different. For scenario 4, besides Entisols and Alfisols, Vertisols are also dominating among the major land cover types. According to the definition by ("The Twelve Orders of Soil Taxonomy", n. d.), Vertisols transmit water very slowly and have little leaching undergone its soil layers. Therefore, soil types in Scenario 4 seem to perform better when it comes to water holding capacities. Consequently, although the land cover types dominate among shallow-rooted plants such as grass or crops, scenario 4 has shown a better tolerance or insensitivity to the soil moisture changes than scenario 3.

Samples with the highest R^2 values at SM (9-7_1) time lag (Figure 13 and 14) occurred under grasslands and croplands, with Alfisols (Table 10 and 11), thus further showing land covers with shallow-rooted vegetation and soil type with high water holding capacity are highly associated with soil moisture memory effects.

5.4 Memory effects within the context of Land surface-atmosphere feedbacks

The mem7-9 found in this paper is relatively uniform across Sahel at continental level, nevertheless, only a few samples from the selected sample points have shown a different memory effect in time between NDVI residuals and soil moisture content. The impact of these memory effects on the climate can be analysed through studying the land surface-atmosphere feedbacks.

According to the paper by Philippon et al. in 2005, an inter-season memory effect in the Guinean region is discovered under effectiveness from autumn to spring between precipitation and soil-vegetation water content. Moreover, the West African monsoon is driven by the meridional gradient of entropy that develops between

the tropical South Atlantic and the subcontinent. Such a gradient can be partially controlled by soil-vegetation water content anomalies observed in the paper by Philippon et al, at inter-annual and intra-annual time scales. The observed spring soil-vegetation water content anomalies therefore strengthen the meridional gradient of soil-vegetation water content over the subcontinent, which as a result will also strengthen the West African monsoon (Philippon et al, 2005).

Thus, inter-seasonal memory effects such as the one found in this paper could conceivably play a role in the Sahelian precipitation variability while influencing the meridional gradient of soil-vegetation water content which drives the West African monsoon.

Los et al. (2006) compared the model of NDVI, which contains dependent variables of precipitation and surface air temperature, both with values from concurrent month plus previous two months, with the NDVI model which contains three additional variables, including vegetation and climate feedbacks, precipitation and temperature, and a one year vegetation memory feedback. Results have shown that NDVI as a dependent variable can be well explained by memory effects at annual time scales and feedback effects at monthly time scales. Furthermore, annual precipitation can be well explained if vegetation-precipitation feedback is included in the multi-linear regression model. Results from the integrated model have indicated that the vegetation feedback increases the variance in annual precipitation by at least 30% in Sahel, especially during the month of July and August when the inter-tropical convergence zone (ITCZ) moves northward (Los et al, 2006). To conclude, annual memory effect of vegetation is found to play a role in explaining the seasonal and inter-annual variability in vegetation greenness, nevertheless, vegetation greenness if integrated into the model for inter-annual precipitation, can explain its variability by at least 30%. Therefore, same theory could also be applied in this study that memory effect such as mem7-9 could impose an indirect force onto the annual precipitation, thus contribute to the land surface-atmosphere feedbacks.

5.5 Uncertainties

Areas with significant R^2 or r values, such as sample 4a (R^2=0.48) and sample 8b (R^2=0.39), have indicated the influence of a memory effect between SM with time lags and NDVI over the raining season, thus indicating SM with time lags is the dominant causative factor for explaining NDVI anomalies. However, the unexplained NDVI variables (or residuals) presented in the linear models implied that there are factors other than the SM with time lags also played an part in

explaining the NDVI anomalies. Potential factors such as human impacts (i.e. changes in land use, exploitation of natural resources) are hypothesized by Hermann et al. in 2005. However, various factors including natural and anthropogenic, are still unknown within the context of this study, and can be studied in the future.

The temporal resolution (yearly) as well as spatial resolution (8*8 km) of the NDVI and SM data sets used in this study can impose potential risk of missing information within the processes of linear regression analysis. By using 10-day composites, Justice et al (1991) have indicated a 10-to-20 day time lags for correlations between rainfall and NDVI in Sahel. Moreover, by using half-hourly in-situ rainfall and soil moisture measurements between year 2005 and 2009, Jamali et al (2011) have discovered that vegetation indices (NDVI and EVI) related to soil moisture of the upper 1m by 0-28 days at sub-Saharan sites. Notice that the dependent variable in this study is NDVI residuals calculated from the linear model, therefore there is a little bit difference between the correlation results in this study than the ones mentioned above. However, with correlation between data sets at yearly level, uncertainties do exist and cannot be ignored.

Furthermore, the soil map adopted in this study is converted from the FAO Soil Map of the World, and soil climate map. Thus a conversion will require assigning suborder to every combination of FAO classification and soil climate map. However, direct correlations are not always available for such a conversion, therefore might impose uncertainties for certain area or class. For the Global Land Cover 2000 Map, accuracy assessment done by Mayaux et al. (2006) has indicated an accuracy of 68.6%, which is relatively good but still imply the existence of uncertainties.

5.6 Future Work

The Study area can be narrowed down to only include Sahel region with the lineation over the four eco-climatic zones defined by FAO.

Instead of using the whole time series data sets of NDVI and soil moisture, it might be more interesting to study the NDVI and soil moisture relationship by diving between the wet and dry years. If the wet and dry years are not differentiated, NDVI residuals obtained from the linear models should then be separated according to their positive and negative values, and correlate with trimestral soil moisture content respectively. Thus, these lag effects can be further differentiated as memory effects from the wet years and recovery effects from the dry years.

The linear model between NDVI and SM over the raining season has shown high correlation coefficients (with maximum r=0.88 & -0.70), however, the unexplained variables can be further explained if the linear model between NDVI and SM is constructed using all-season data (Huber et al., 2011).

The method used in this study for identifying memory effects are based on the work by Richard et al. in 2008, however its validity is never assessed. Therefore, field work data can be collected and used as the validation source to assess the identified memory effect according to the linear model between NDVI residuals and SM with time lags.

The Granger causality method or the distributed lagged model could be used as potential candidate to further improve the simple linear model between NDVI and SM time series data.

Chapter 6: Conclusion

This study has been able to identify a memory effect of 7-to-9 month time lag between soil moisture data and NDVI time series at a sub-continental level. Spatial distributions of the above-normal and below-normal NDVI residuals with high sensitivity to soil moisture content have implied the importance of west Sahel and central to east Sahel (among the countries of Chad, Central African Republic, and Sudan) as the sensitive zones towards soil moisture changes.

Furthermore, this study has revealed associations of the memory effect with land cover and soil type. Results have shown land covers with crops and open grassland with sparse shrubs are more sensitive to soil moisture changes than shrubs or trees. Thus, a high content in soil moisture 7-to-9 months ago will stimulate vegetation (grasses or crops) growth in the up-coming spring, and vice versa. Another interesting result from the study is associated with soil types with high water-holding capacities, such as Alfisols and Vertisols, if presenting in the environment, will keep the shallow-rooted plants (i.e. Crops and grasses) being tolerant to low soil moisture content 7-to-9 months ago, especially in the dry years.

In overall, an inter-annual memory effect between soil moisture and NDVI had been identified in this study. By integrating the memory effects with land cover types and soil types, it explains the underlying mechanisms of environmental factors which stimulate the memory effect. Therefore, it will be interesting to study the memory effect on small scales, selected by different land covers and soil types. Thus, each study area with uniformed land cover and soil type will reflect its memory effect with less spatial heterogeneity, therefore, more accuracy.

References

Ahmed, M. (2012). Significance of soil moisture on vegetation greenness in the African Sahel from 1982 to 2008. Unpublished master thesis for master's degree, Lund University, Lund, Sweden.

Anyamba, A., & Tucker, C. J. (2005). Analysis of Sahelian vegetation dynamics using NOAA-AVHRR NDVI data from 1981–2003. Journal of Arid Environments,63(3), 596-614.

Asrar, G., Fuschs, M., Kanemasu, E. T., and Hatfield, J. L., (1984). Estimating absorbed photosynthetic radiation and leaf area index from spectral reflectance in wheat. Agronomy Journal, Vol. 76, pp. 300–306.

Bader, J., & Latif, M. (2003). The impact of decadal□scale Indian Ocean sea surface temperature anomalies on Sahelian rainfall and the North Atlantic Oscillation. Geophysical Research Letters, 30(22).

Brooks, N., 2004. Drought in the African Sahel: Long term perspectives and future prospects. Tyndall Centre Working Papers, 61, http://www.tyndall.ac.uk/sites/default/files/wp61.pdf (April, 2013).

Brooks, N., (2006). Climate Change, drought and pastoralism in the Sahel. Discussion note for the World Initiative on Sustainable Pastoralism, http://cmsdata.iucn.org/downloads/e_conference_discussion_note_for_the_world_initiative_on_sustainable_pastoralism_.pdf (May 28, 2013).

Cook, K. H., & Vizy, E. K. (2006). Coupled model simulations of the West African monsoon system: Twentieth-and twenty-first-century simulations.Journal of climate, 19(15), 3681-3703.

Climatic extremes, from drought to flood, threaten survival. (2010). In The Economist. Retrieved from http://www.economist.com/node/17628093.

Fan, Y., & van den Dool, H. (2004). Climate Prediction Center global monthly soil moisture data set at 0.5 resolution for 1948 to present. Journal of Geophysical Research: Atmospheres (1984–2012), 109(D10).

FAO/GIEWS (Food and Agriculture Organization of the United Nations/ Global Information and Early Warning System), (1998). Sahel Report No. 1, Sahel weather and crop situation 1998
http://www.fao.org/giews/english/sahel/index.htm [accessed 28/05/2013].

FAO/GIEWS (Food and Agriculture Organization of the United Nations/ Global Information and Early Warning System), (2007). Sahel Report No. 3,

Galbraith, S., Daniel, J. A., & Vissel, B. (2010). A study of clustered data and approaches to its analysis. The Journal of Neuroscience, 30(32), 10601-10608.

Giannini, A., Saravanan, R. and Chang, P., (2003). Oceanic Forcing of Sahel Rainfall on Interannual to Interdecadal Time Scales. Science, 302, 1027-1030.

Giannini, A., Biasutti, M., Held, I. M., & Sobel, A. H. (2008a). A global perspective on African climate. Climatic Change, 90(4), 359-383.

Giannini, A., Biasutti, M., & Verstraete, M. M. (2008b). A climate model-based review of drought in the Sahel: Desertification, the re-greening and climate change. Global and planetary Change, 64(3), 119-128.

GIMMS data documentation, http://glcf.umiacs.umd.edu/data/gimms/index.shtml [accessed 20/10/2012]

Gonzalez, P., (2001). Desertification and a shift of forest species in the West African Sahel.Climate Research, 17, 217-228.

Griffiths, J. F. (1972). Climates of Africa, Vol. 10 of World Survey of Climatology.

Hagos, S. M., & Cook, K. H. (2008). Ocean warming and late-twentieth-century Sahel drought and recovery. Journal of Climate, 21(15), 3797-3814.

Hansen, J., Lacis, A., Rind, D., Russel, G., Stone, P., Fung, I., Ruedy, R. and Lerner, J., (1984). Climate sensitivity: Analysis of feedback mechanisms. In: Hansen, J. and Takahashi, T.(eds.) Climate Processes and Climate Sensitivity. Washington, D. C., Geophysical Monograph 29, American Geophysical Union. (130-163 p).

Held, I. M., Delworth, T. L., Lu, J., Findell, K. L., & Knutson, T. R. (2005). Simulation of Sahel drought in the 20th and 21st centuries. Proceedings of the National Academy of Sciences of the United States of America, 102(50), 17891-17896.

Herrmann, S.M., Anyamba, A. and Tucker, C. J., (2005). Recent trends in vegetation dynamics in the African Sahel and their relationship to climate. Global Environmental Change-Human and policy Dimensions, Vol.15, No.4, pp. 394–404.

Heumann, B. W., Seaquist, J. W., Eklundh, L., & Jönsson, P. (2007). AVHRR derived phenological change in the Sahel and Soudan, Africa, 1982–2005.Remote Sensing of Environment, 108(4), 385-392.

Hickler, T., Eklundh, L., Seaquist, J. W., Smith, B., Ardö, J., Olsson, L., & Sjöström, M. (2005). Precipitation controls Sahel greening trend. Geophysical Research Letters, 32(21), L21415.

Hoerling, M., Hurrell, J., Eischeid, J., & Phillips, A. (2006). Detection and attribution of twentieth-century northern and southern African rainfall change.Journal of climate, 19(16), 3989-4008.

Huber, S., Fensholt, R., & Rasmussen, K. (2011). Water availability as the driver of vegetation dynamics in the African Sahel from 1982 to 2007. Global and Planetary Change, 76(3), 186-195.

Hulme, M., Doherty, R., Ngara, T., New, M. and Lister, D., (2001). African climate change: 1900-2100. Climate Research, 17, 145-168.

IPCC (Intergovernmental Panel on Climate Change), (2001). Climate Change 2001: Impacts, Adaptation & Vulnerability: Contribution of Working Group II to the Third Assessment Report of the IPCC, J. J. McCarthy, O. F. Canziani, N. A. Leary, D. J. Dokken and K. S. White, eds. Cambridge University Press, Cambridge, UK, 1032 pp.

Jamali, S., Seaquist, J. W., Ardö, J., & Eklundh, L. (2011). Investigating temporal relationships between rainfall, soil moisture and MODIS-derived NDVI and EVI for six sites in Africa. Savanna, 21, 547.

Justice, C. O., Dugdale, G., Townshend, J. R. G., Narracott, A. S., & Kumar, M. (1991). Synergism between NOAA-AVHRR and Meteosat data for studying vegetation development in semi-arid West Africa. International Journal of Remote Sensing, 12(6), 1349-1368.

Klönne, U. (2012). Drought in the Sahel –global and local driving forces and their impact on vegetation in the 20th and 21st century, Lund University, Lund, Sweden.

Lamb, P.J., (1982). Persistence of Sub-Saharan drought. Nature, Vol. 299, pp. 46–48.

Le Houerou, H.N., (1980). The range lands of the Sahel. Journal of Range Management, Vol.33, 41–46.

Los, S. O., Weedon, G. P., North, P. R. J., Kaduk, J. D., Taylor, C. M., & Cox, P. M. (2006). An observation□based estimate of the strength of rainfall□vegetation interactions in the Sahel. Geophysical research letters, 33(16).

Martiny, N., Richard, Y., & Camberlin, P. (2005). Interannual persistence effects in vegetation dynamics of semi□arid Africa. Geophysical research letters,32(24).

Mayaux, P., Eva, H., Gallego, J., Strahler, A. H., Herold, M., Agrawal, S., & Roy, P. S. (2006). Validation of the global land cover 2000 map. Geoscience and Remote Sensing, IEEE Transactions on, 44(7), 1728-1739.

Maynard, K., Royer, J. F., & Chauvin, F. (2002). Impact of greenhouse warming on the West African summer monsoon. Climate Dynamics, 19(5-6), 499-514.

Motha, R. P., Leduc, S. K., Steyaert, L. T., Sakamoto, C. M., & Strommen, N. D. (1980). Precipitation patterns in west Africa. Monthly Weather Review,108(10), 1567-1578.

Moustakas, A., Wiegand, K., Meyer, K. M., Ward, D., & Sankaran, M. (2010). perspective: Learning new tricks from old trees: revisiting the savanna question.Frontiers of Biogeography, 2(2).

Mulford, M R. (1994). In Government, Population and Ecology in the Sahel: a Study in Disaster. Retrieved from http://www.frontiernet.net/~mmulford/sahel.htm.

United States Department of Agriculture, Natural Resources Conservation Service. (n.d.). The Twelve Orders of Soil Taxonomy. Retrieved from http://soils.usda.gov/technical/soil_orders/

Nemani R.R., Keeling C.D., Hashimoto H., Jolly W.M., Piper S.C., Tucker C.J., Myneni R.B. and Running S.W., (2003). Climate driven increases in global terrestrial net primary production from 1982 to 1999. Science, Vol. 300, pp. 1560–1563.

Nicholson, S. E., Davenport, M. L., & Malo, A. R. (1990). A comparison of the vegetation response to rainfall in the Sahel and East Africa, using normalized difference vegetation index from NOAA AVHRR. Climatic Change, 17(2-3), 209-241.

Nicholson, S. E., Tucker, C. J., & Ba, M. B. (1998). Desertification, drought, and surface vegetation: An example from the West African Sahel. Bulletin of the American Meteorological Society, 79(5), 815-829.

Olsson, L., Eklundh, L., & Ardö, J. (2005). A recent greening of the Sahel—trends, patterns and potential causes. Journal of Arid Environments, 63(3), 556-566.

Paeth, H. and Hense, A., (2004). SST versus climate change signals in West African rainfall: 20thcentury variations and future projections. *Climatic Change*, 65, 179-208.

Philippon, N., Mougin, E., Jarlan, L., & Frison, P. L. (2005). Analysis of the linkages between rainfall and land surface conditions in the West African monsoon through CMAP, ERS□WSC, and NOAA□AVHRR data. *Journal of Geophysical Research: Atmospheres* (1984–2012), 110(D24).

Richard, Y., Martiny, N., Fauchereau, N., Reason, C., Rouault, M., Vigaud, N., & Tracol, Y. (2008). Interannual memory effects for spring NDVI in semi□arid South Africa. *Geophysical Research Letters*, 35(13), L13704

Richard, Y., Martiny, N., Rouault, M., Philippon, N., Tracol, Y., & Castel, T. (2012). Multi-month memory effects on early summer vegetative activity in semi-arid South Africa and their spatial heterogeneity. *International Journal of Remote Sensing*, *33*(21), 6763-6782.

Schenk, H. J., & Jackson, R. B. (2002). Rooting depths, lateral root spreads and below□ground/above□ground allometries of plants in water□limited ecosystems. *Journal of Ecology*, 90(3), 480-494.

Seaquist, J. W., Hickler, T., Eklundh, L., Ardo, J., & Heumann, B. W. (2009). Disentangling the effects of climate and people on Sahel vegetation dynamics.*Biogeosciences*, *6*(3), 469-477.

Sjöström M., Ardö J., Eklundh L., El-Tahir B.A., El-Khidir H.A.M., Hellström M., Pilesjö P. and Seaquist J., (2009). Evaluation of satellite based indices for gross primary production estimates in a sparse savanna in the Sudan. *Biogeosciences*, Vol. 6, No.1, pp. 129-138.

The Sahel Crisis. (2013). In *Food and Agriculture Organization of the United Nations*. Retrieved from http://www.fao.org/crisis/sahel/en/

Tucker, C. J., Vanpraet, C., Sharman, M. J., and Van Ittersum, G., (1985). Satellite remote sensing of total herbaceous biomass production in the Senegalese Sahel: 1980-1984. *Remote Sensing of Environment*, Vol. 17, No. 3, pp. 233- 249.

Vanacker, V., Linderman, M., Lupo, F., Flasse, S. and Lambin, E. F., (2005). Impact of short-term rainfall fluctuation on interannual land cover change in sub-Saharan Africa. *Global Ecology and Biogeography*, 14, 123-135.

Yoshioka, M., Mahowald, N. M., Conley, A. J., Collins, W. D., Fillmore, D. W., Zender, C. S., & Coleman, D. B. (2007). Impact of desert dust radiative forcing on Sahel precipitation: Relative importance of dust compared to

sea surface temperature variations, vegetation changes, and greenhouse gas warming.*Journal of Climate*, *20*(8), 1445-1467.

Zeng, N., Neelin, J. D., Lau, K. M., & Tucker, C. J. (1999). Enhancement of interdecadal climate variability in the Sahel by vegetation interaction. *Science*,*286*(5444), 1537-1540.

Appendix

Appendix 1. R^2 from linear regression models between NDVI residuals and soil moistures with time lags, over samples selected from Figure (9a)

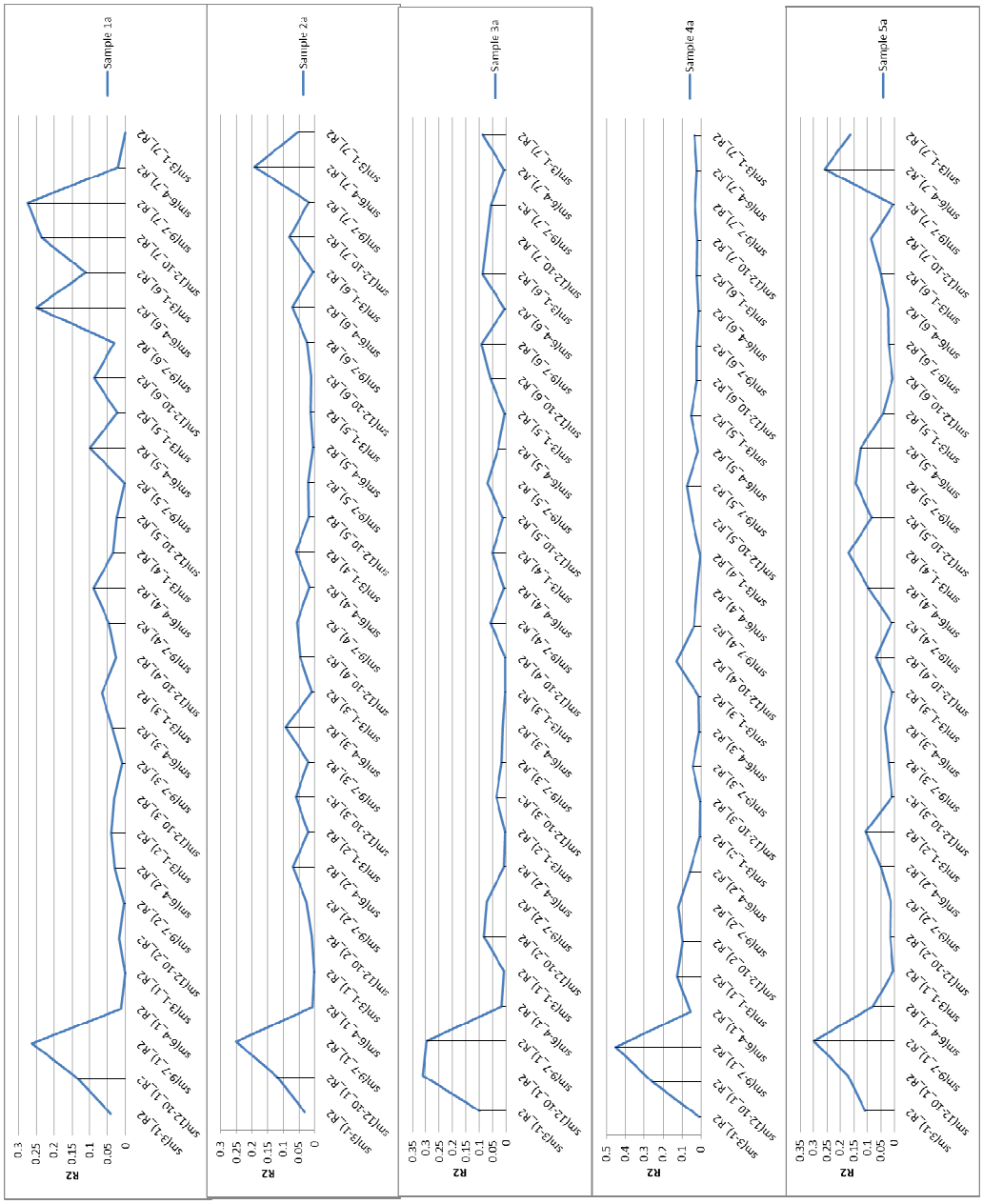

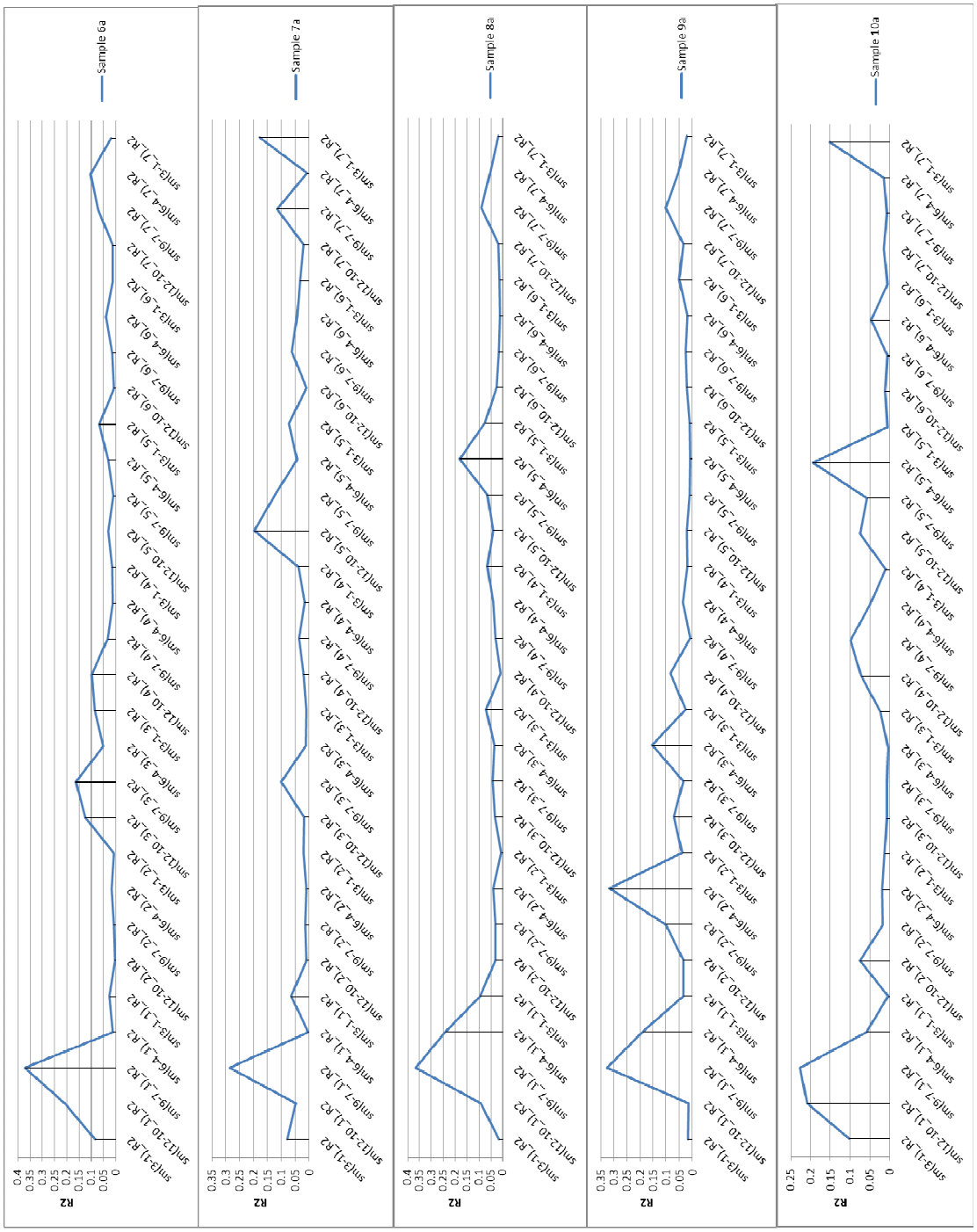
Sample 6a
Sample 7a
Sample 8a
Sample 9a
Sample 10a
R2

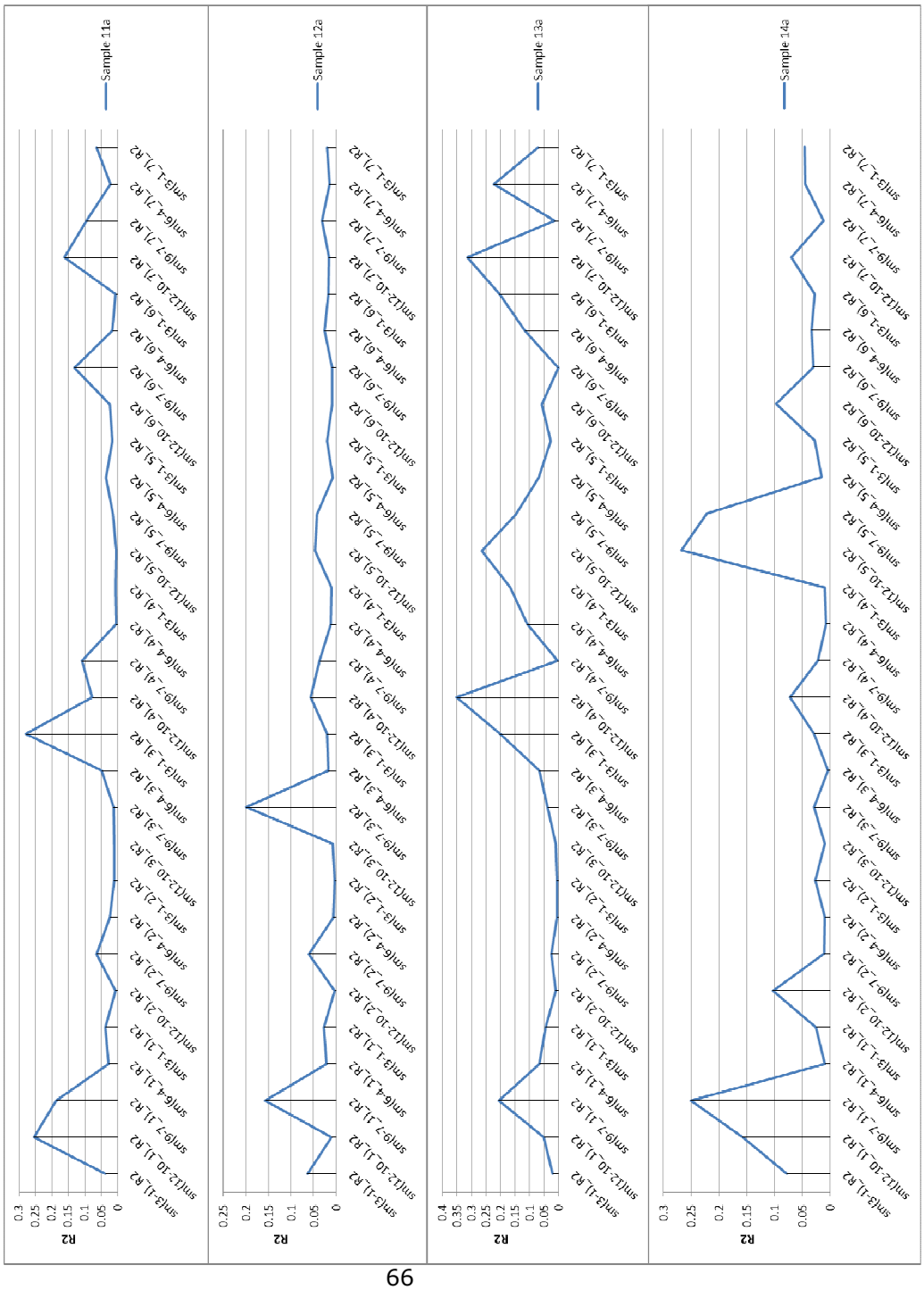
Sample 11a
Sample 12a
Sample 13a
Sample 14a
R2

Appendix 2.

R^2 from linear regression models between NDVI residuals and soil moistures with time lags, over samples selected from Figure (9b)

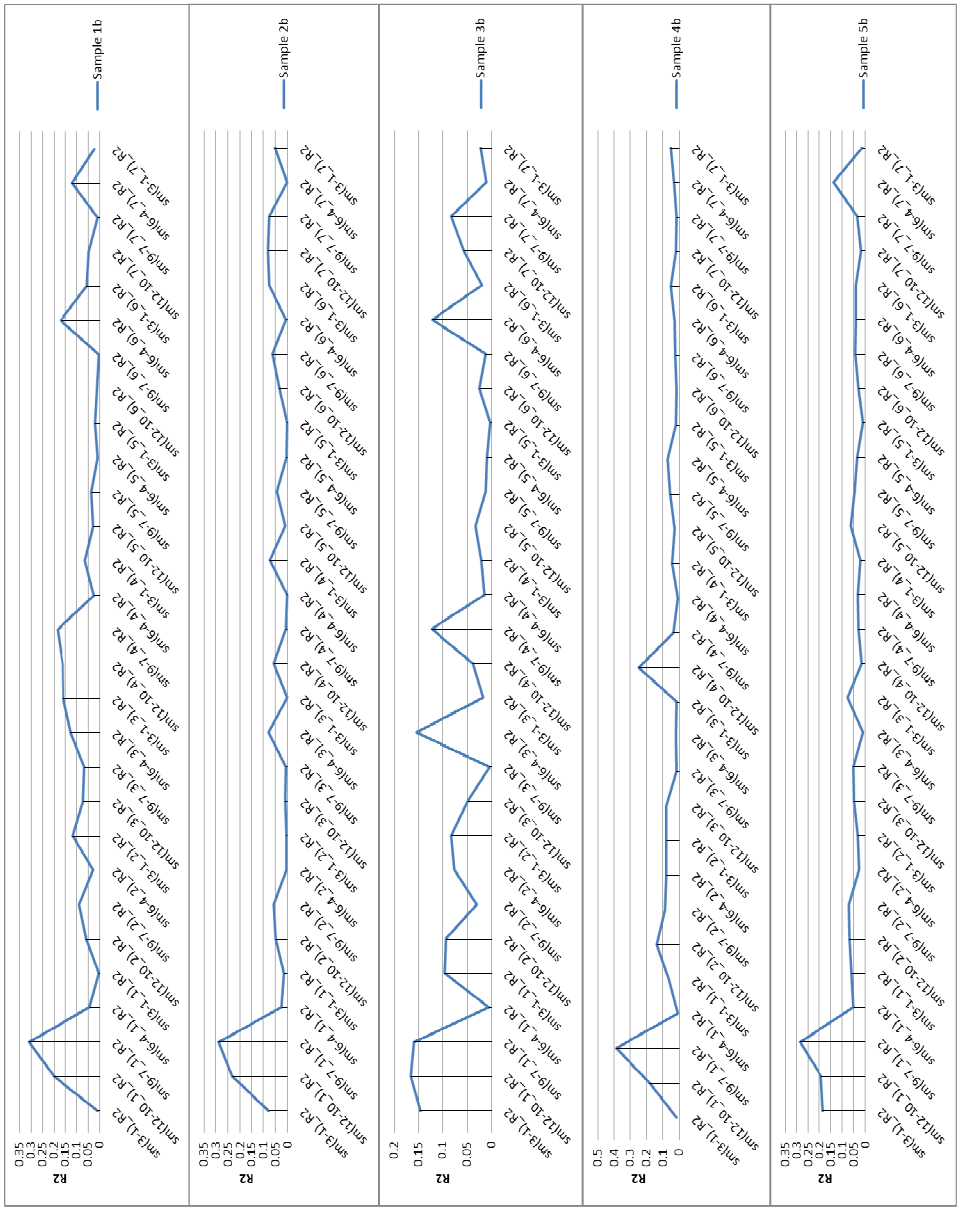

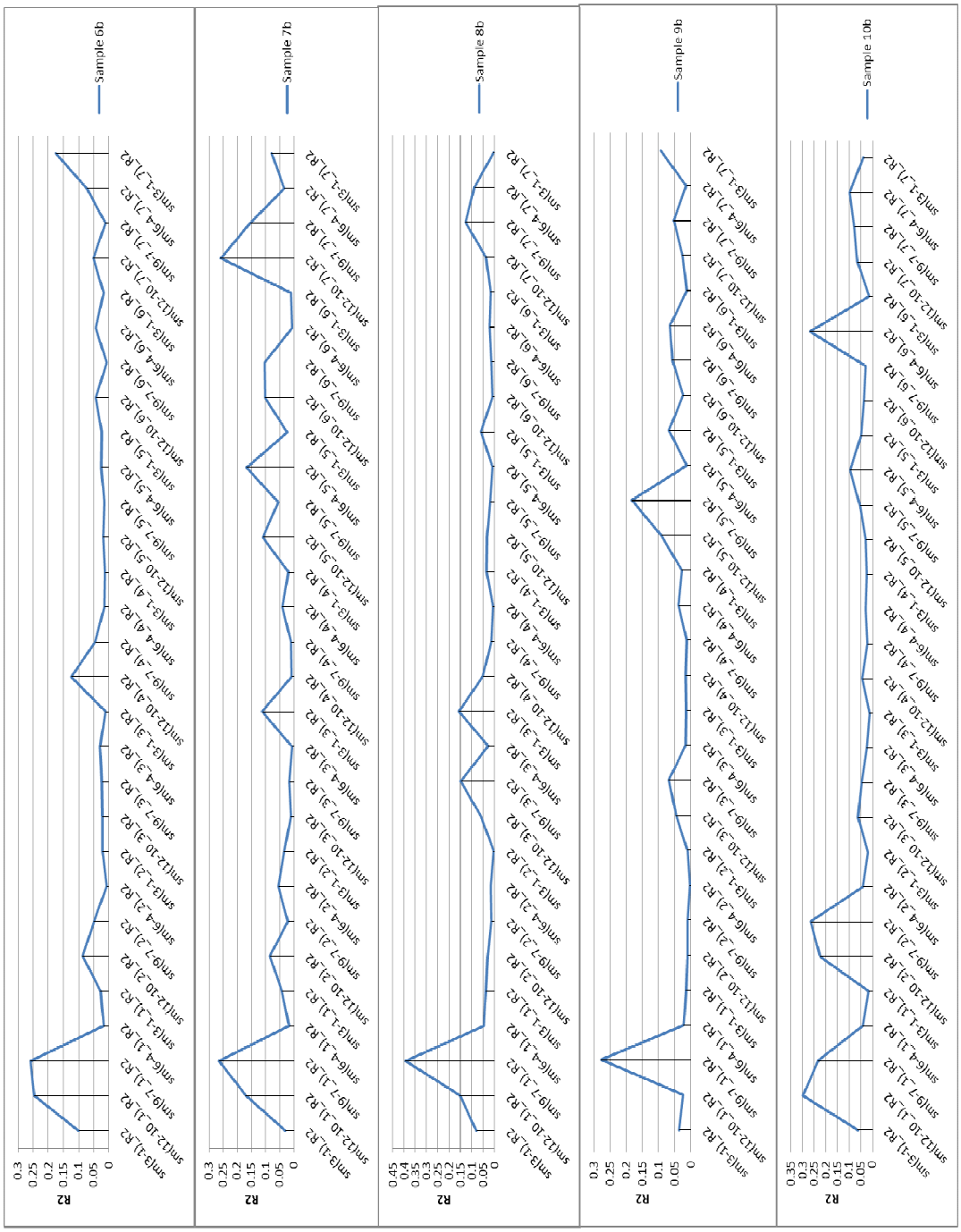
Sample 6b
Sample 7b
Sample 8b
Sample 9b
Sample 10b
R2

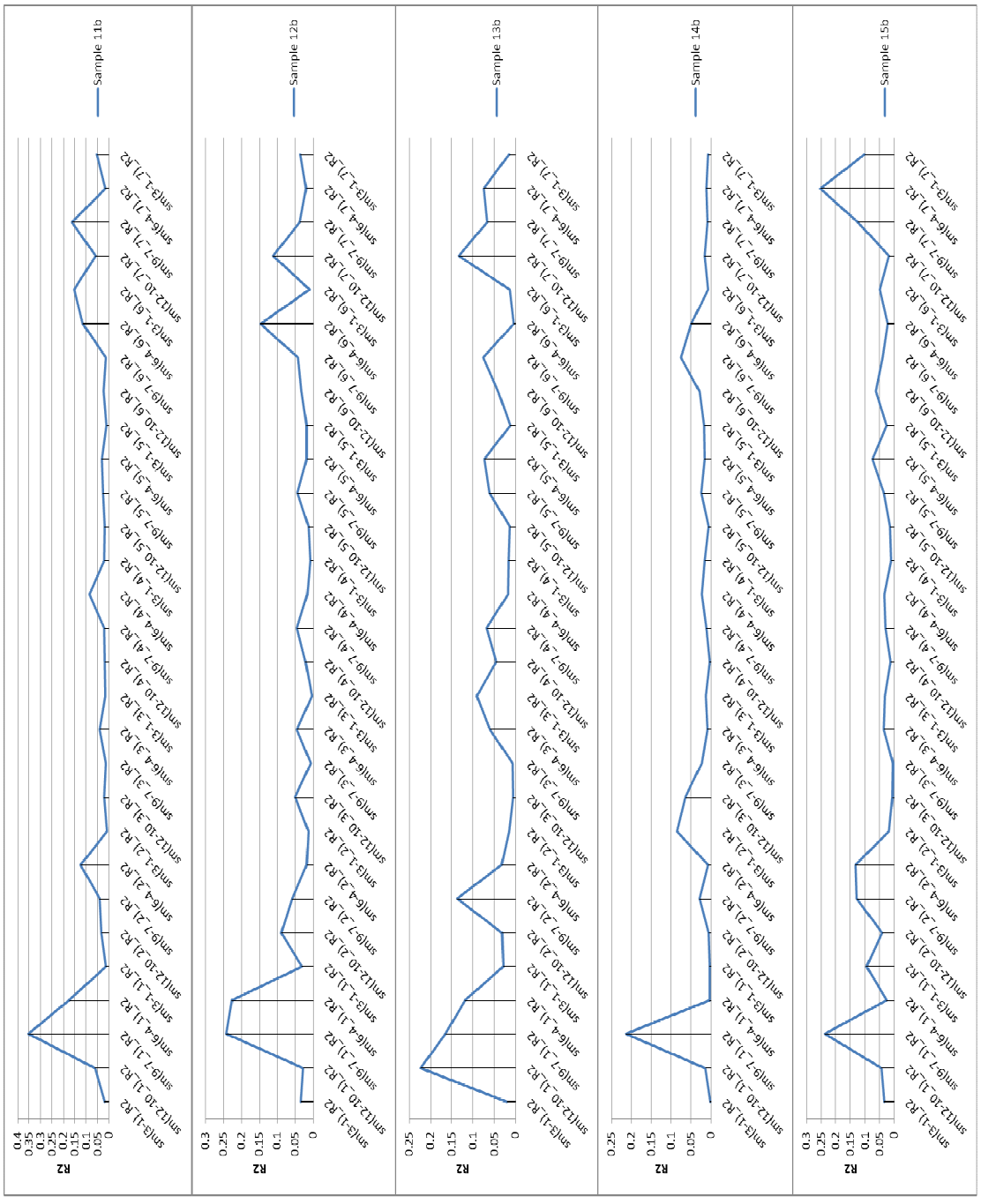
Sample 11b
Sample 12b
Sample 13b
Sample 14b
Sample 15b
R2

Department of Physical Geography and Ecosystem Science, Lund University

Lund University GEM thesis series are a series of master theses written by students of the international master program on Geo-information Science and Earth Observation for Environmental Modelling and Management (GEM). The program is a cooperation of EU universities in Iceland, the Netherlands, Poland, Sweden and UK, as well a partner university in Australia. In this series only master thesis are included of students that did their project at Lund University. Other theses of this program are available from the ITC, the Netherlands (www.gem-msc.org or www.itc.nl).

The student thesis reports are available at the Geo-Library, Department of Physical Geography and Ecosystem Science, University of Lund, Sölvegatan 12, S-223 62 Lund, Sweden. Report series started 2013. The complete list and electronic versions are also electronic available at the LUP student papers (www.nateko.lu.se/masterthesis) and through the Geo-library (www.geobib.lu.se).

1 Soheila Youneszadeh Jalili (2013) The effect of land use on land surface temperature in the Netherlands
2 Oskar Löfgren (2013) Using Worldview-2 satellite imagery to detect indicators of high species diversity in grasslands
3 Yang Zhou (2013) Inter-annual memory effects between Soil Moisture and NDVI in the Sahel